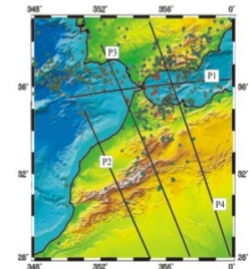
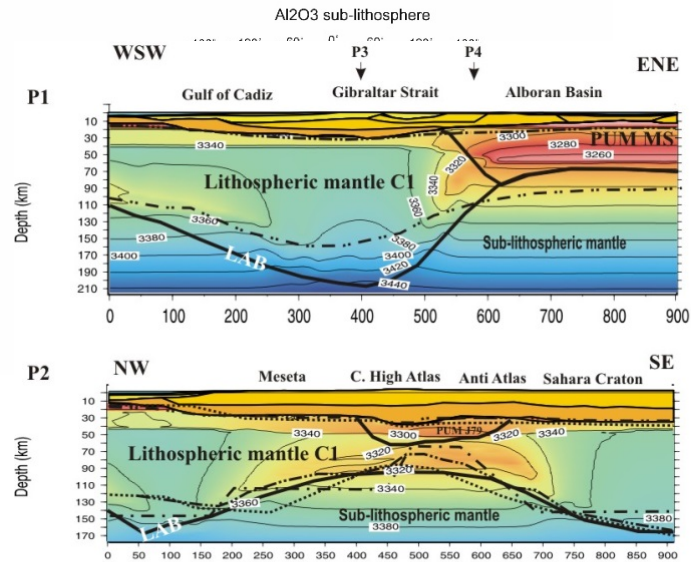
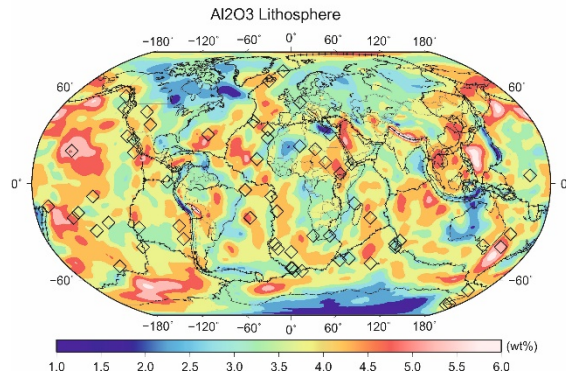
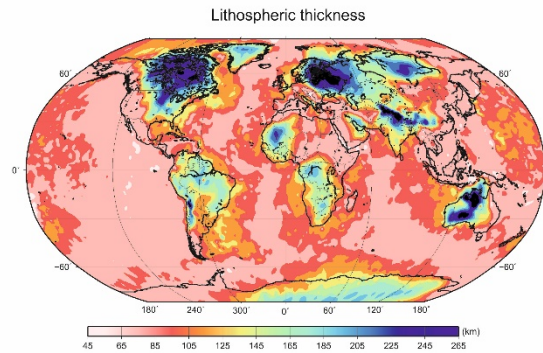
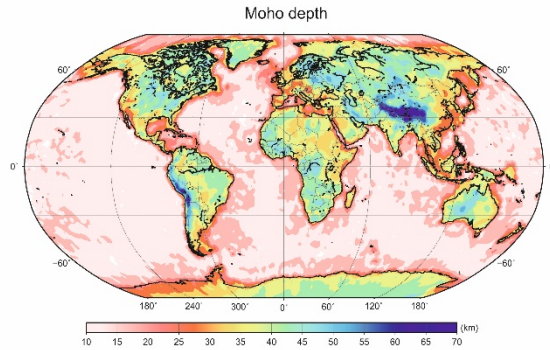


Lithosphere-upper mantle thermochemical modelling at global and regional scale

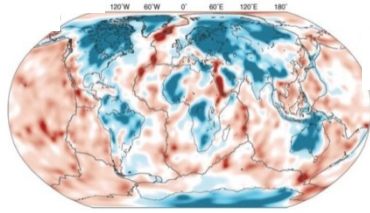


Lithosphere-upper mantle thermochemical structure: why bother?

- ✓ Mantle flow informing plate tectonics: density+ viscosity
- ✓ What supports the Earth's surface topography?
- ✓ Cooling of oceanic lithosphere: half-space vs plate model?
- ✓ Mid Oceanic Ridges: composition, temperature, spreading rate
- ✓ Mantle plumes: temperature and composition
- ✓ Stability of cratonic continental lithosphere

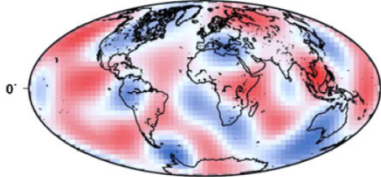
➤ **Many techniques/observations, just ONE Earth...**

Seismic Velocity models



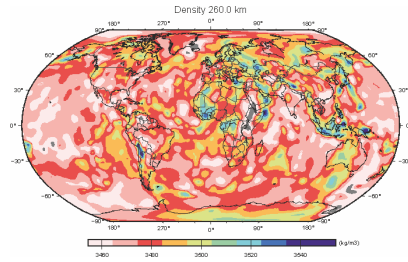
+

Electrical Conductivity models



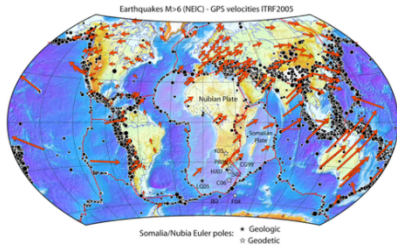
+

Density models



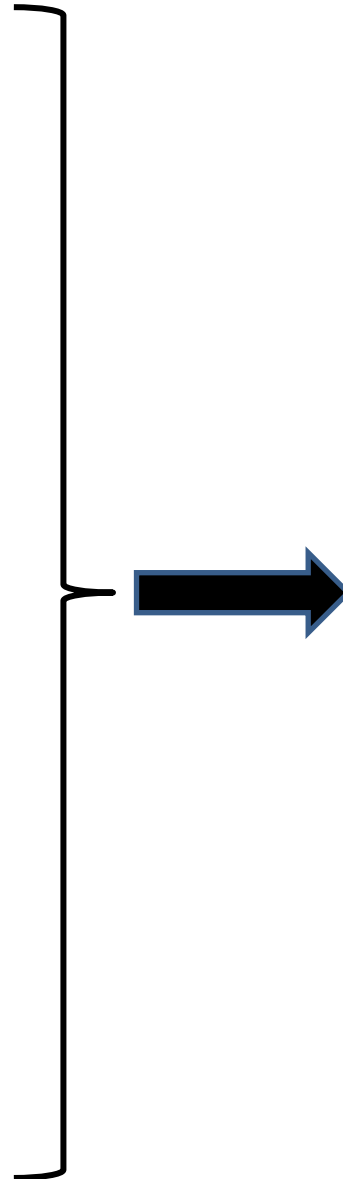
+

Deformation models



+

...



➤ Rock properties → **non linear** functions of thermochemical structure...!



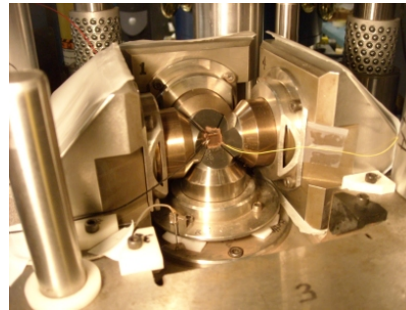
=

$$dG = V dP - S dT + \sum_i \mu_i dX_i$$

+



+



Thermodynamics

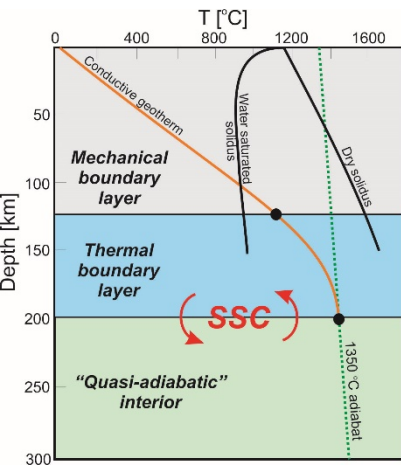
Petrology

Mineral physics

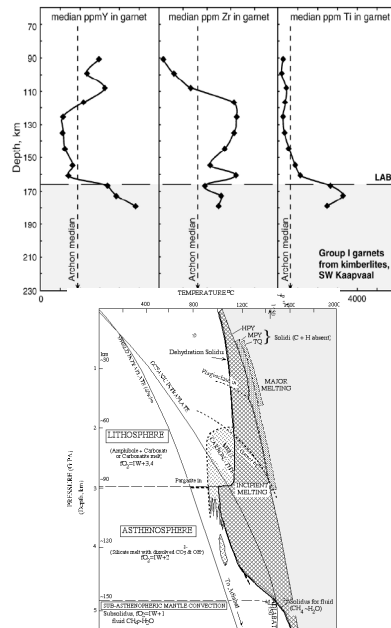
Why integrated modelling...?

A fundamental upper mantle discontinuity for plate tectonics: the lithosphere-asthenosphere boundary (LAB) can be defined as **thermal, mechanical and chemical boundary**.

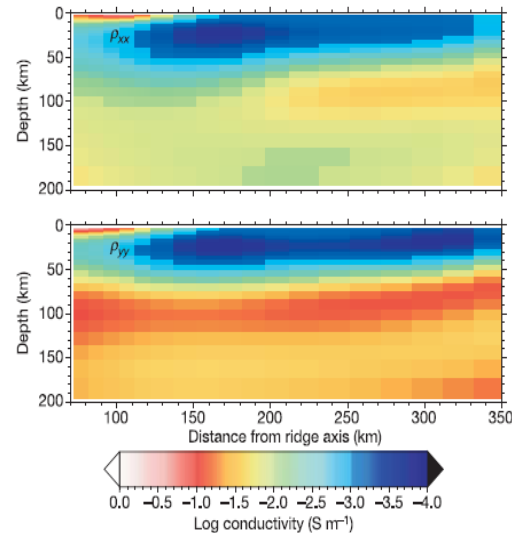
According to the property we focus on (e.g., **temperature, composition, Vs, Vp, anisotropy, electrical conductivity...**) there are many possible “LABs” (e.g. Eaton 2009):



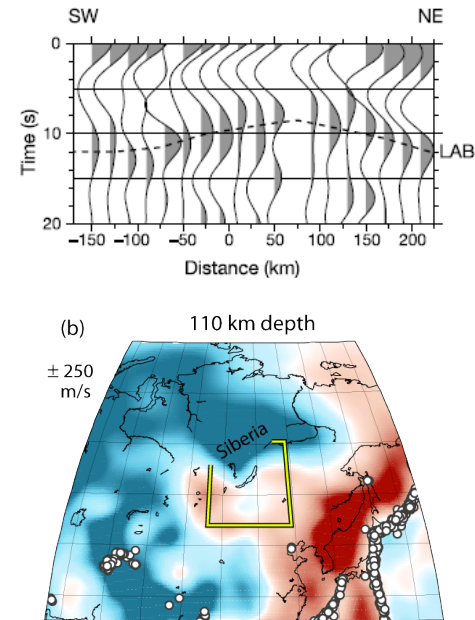
Thermal LAB



**Geochemical/
petrological
LAB**

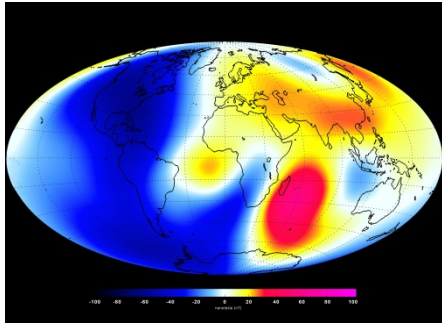


Electric LAB



Seismic LAB

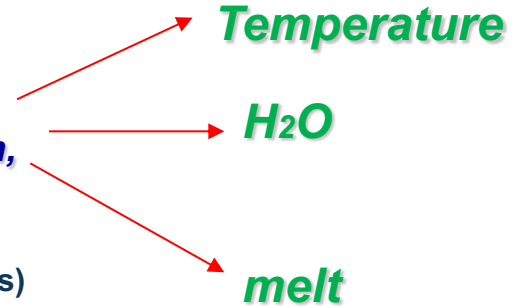
➤ Earth structure: **what** can we know?



Swarm magnetic data
(+ airborne surveys
+observatories and MT)



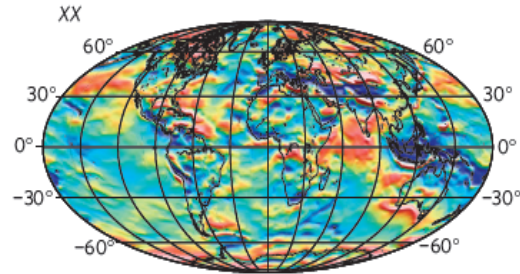
**Electrical
Conductivity,
Curie isotherm,
susceptibility**
(global models
Regional models)



Temperature

H₂O

melt



GOCE gravity data
(+ land gravimetry)

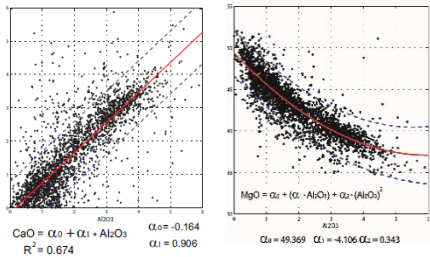


**Density,
Elastic thickness**
(global and
regional models)



Temperature

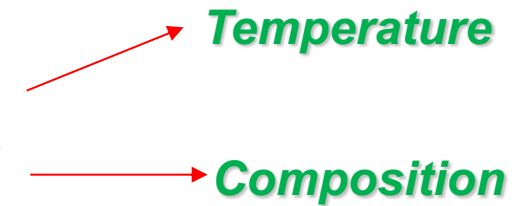
Composition



**World petrological
Data sets**

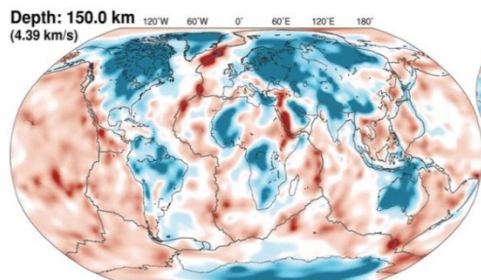


**Thermo-
barometers,
Major oxides
chemistry**



Temperature

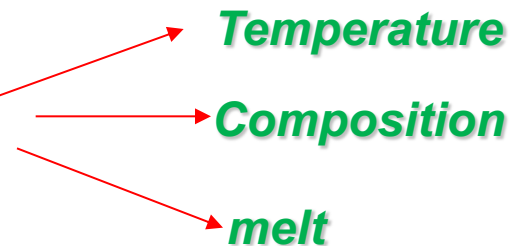
Composition



Seismic tomography
(surface, body waves,
normal modes)



**Seismic
velocities
anisotropy**
(global and
regional models)



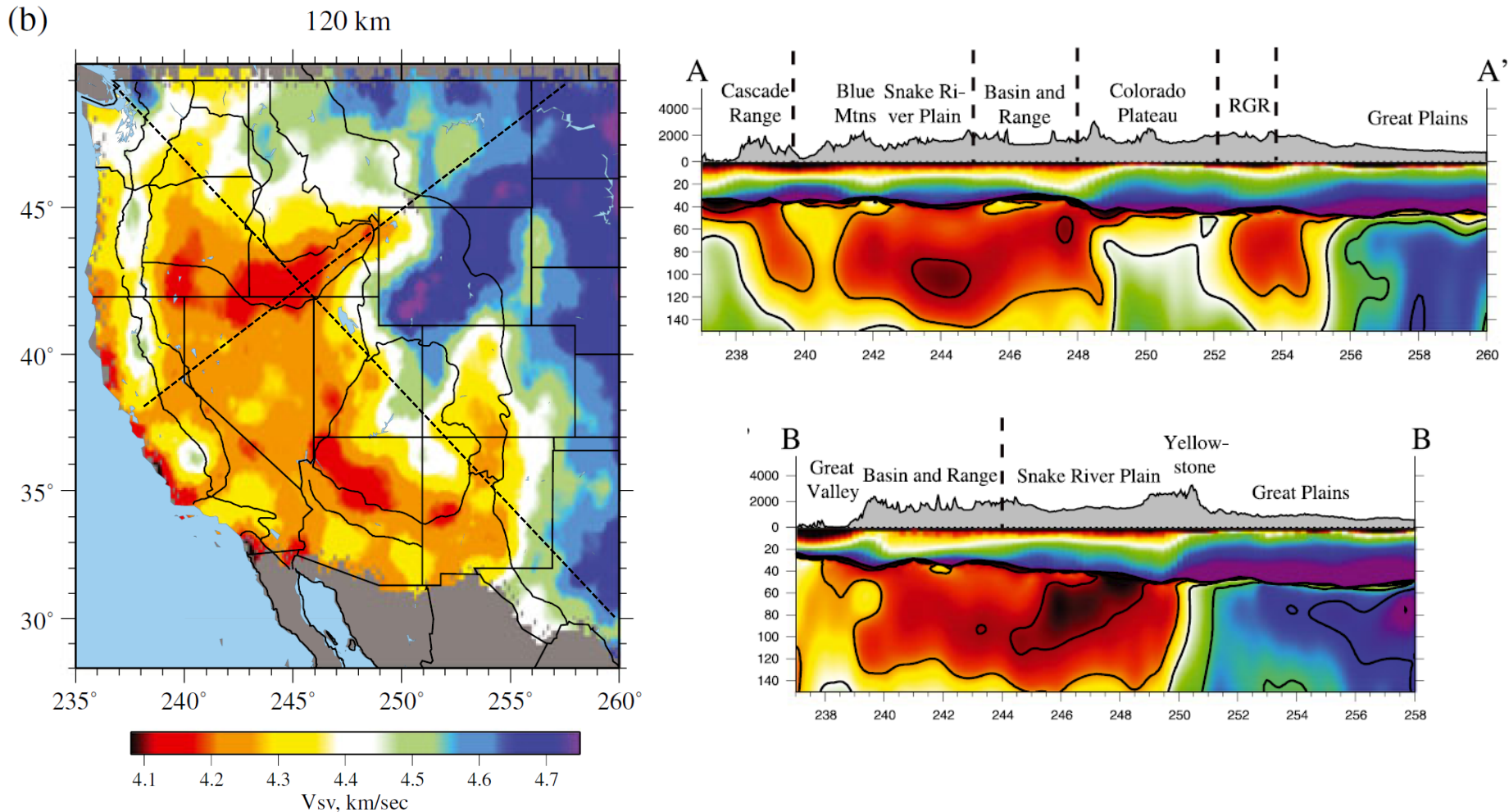
Temperature

Composition

melt

What is the nature of the heterogeneity “observed” in the mantle?

Geophysical point of view



What is the nature of the heterogeneity “observed” in the mantle?

Petrological point of view



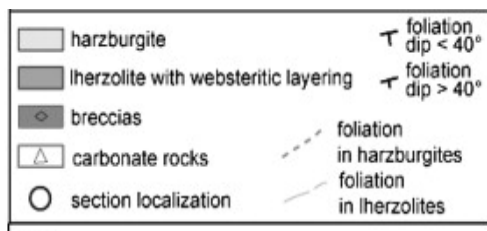
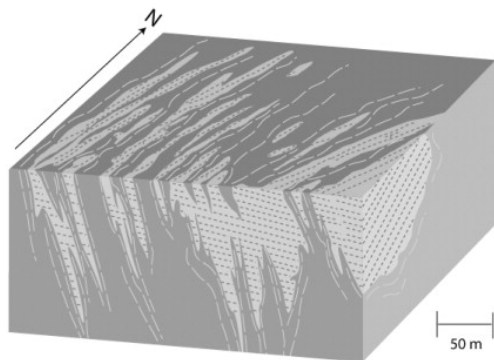
*In mantle
xenoliths*

In outcrops



What is the nature of the heterogeneity “observed” in the mantle?

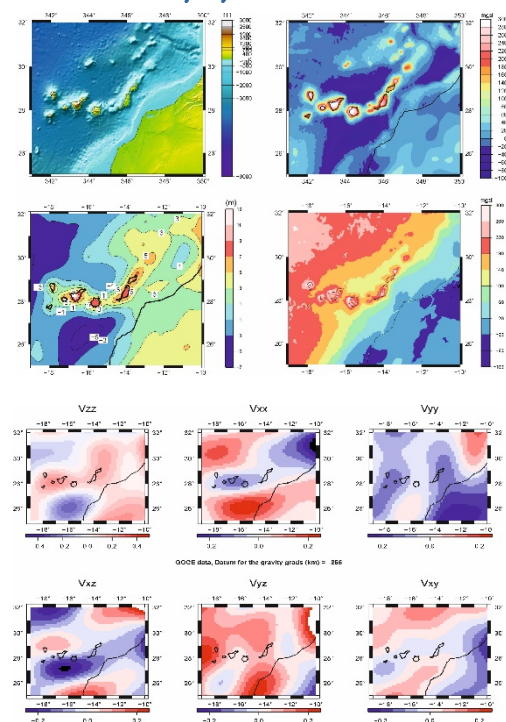
Representativeness of observed mantle samples (xenoliths, peridotite massifs etc..) on the lithospheric scale



Forward modeling



Geophysical data



Depleted

Depleted +metasomatised

	1) Av. Harz. Lanzarote (wt%) ^a	2) Av. HEXO Tenerife (wt%) ^b	3) Av. Harz. La Palma av. (wt%) ^c	4) Av. HLCO Tenerife (wt%) ^b	5) Av. Ocean floor peridot. (wt%) ^d	6) Av. Middle Atlas (wt%) ^e
SiO ₂	43.78	43.32	43.07	42.14	45.09	43.48
Al ₂ O ₃	0.7	0.61	0.53	0.73	2.33	2.38
FeO	7.79	8.04	8.43	8.8	8.4	8
MgO	46.1	45.31	45.19	44.14	41.23	42.6
CaO	0.6	0.81	0.68	1.68	1.32	2.83
Na ₂ O	0.1	0.14	0.17	0.18	0.23	0.24
Mg#	91.34	90.96	90.53	89.94	89.7	90.47

Mantle Depletion (partial melting)

Mantle metasomatism (refertilization)

Mantle Geotherm: thermal lithosphere-asthenosphere boundary

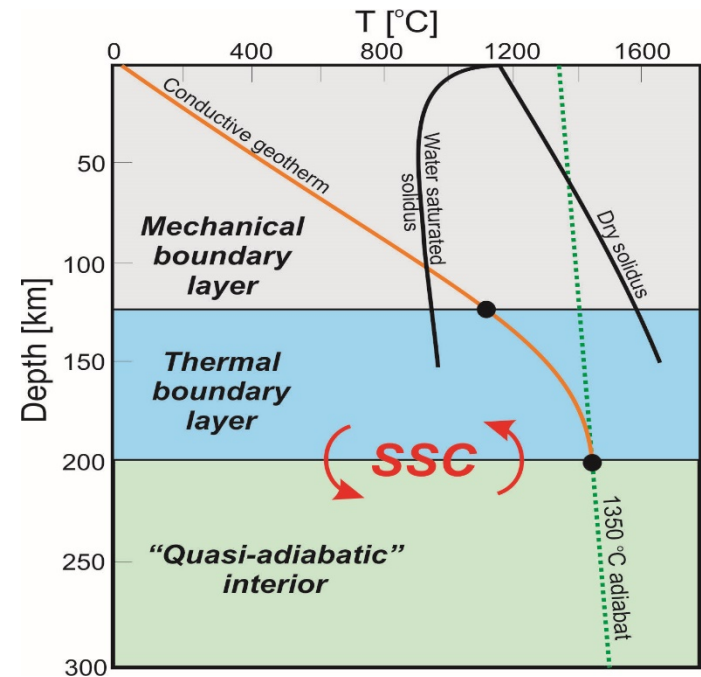
Heat transport equation:

$$\rho c_p \frac{\partial T}{\partial t} = \nabla \cdot (k \nabla T) + H - \rho c_p \vec{u} \cdot \nabla T$$

Lithosphere: conductive mantle

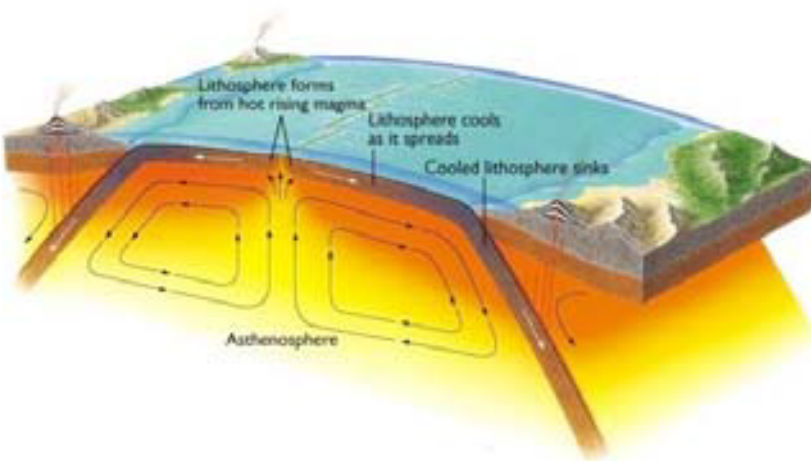
Steady-state conduction equation: $dT/dt=0$
and $U=0 \rightarrow$ Diffusion PDE

$$\nabla \cdot [k(\vec{x}, T, P) \nabla T(\vec{x})] = -H(\vec{x})$$



Sub-Lithosphere: mantle convection

Convection in the mantle (i.e. no heat interexchange with the surroundings). Fast heat transport mechanism compared to conduction



$$\left(\frac{\partial T}{\partial r} \right)_s = \frac{T \alpha g}{c_p}$$

Adiabatic gradient:
typically 0.4-0.5 K/km in
the uppermost mantle

Thermal field

- ✓ Mantle thermal conductivity dependent on T, P and C (numerical iteration)

$$k_{(T,P)} = k^{\circ} \left(\frac{298}{T} \right)^a \exp \left[-(4\gamma + 1/3) \int_{298}^T \alpha(T) dt \right] \times \left(1 + \frac{K'_0 P}{K_T} \right) + k_{rad}(T)$$

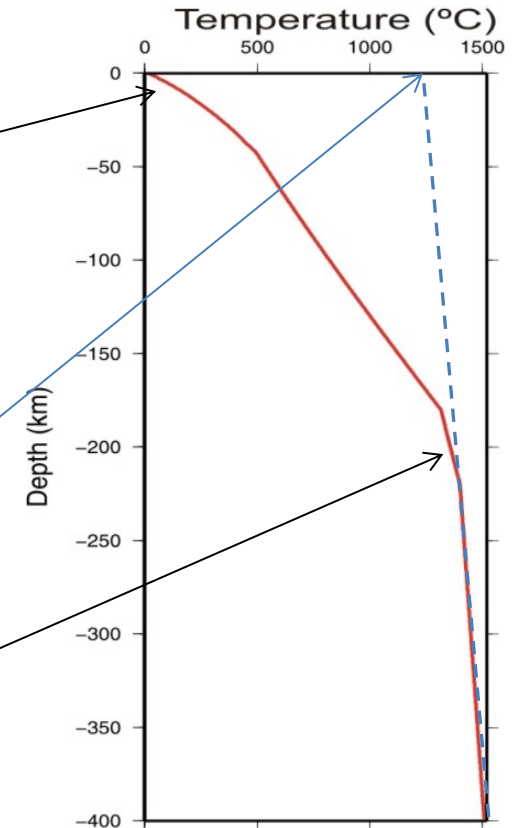
- ✓ Surface Heat flow (SHF) = $Kc \cdot dT/dz$

- ✓ Crustal heat production accounts for 20-40% of SHF in continents

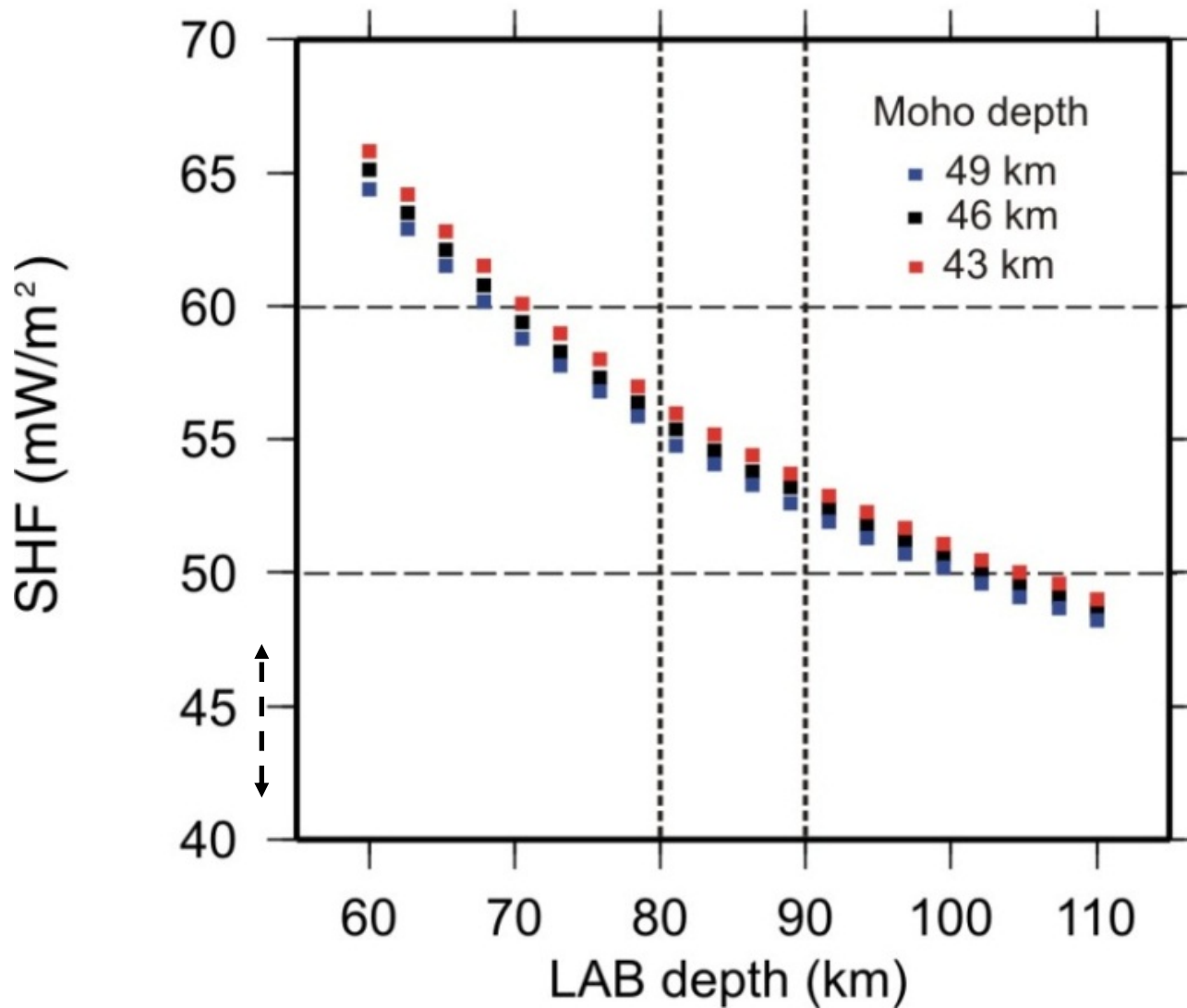
- ✓ Thermal buffer connecting the conductive lithosphere with the adiabatic sublithosphere. $T_{buffer} = 1420 \text{ }^{\circ}\text{C}$ (mantle potential temperature of $1350 \text{ }^{\circ}\text{C}$)

- ✓ Sublithospheric geotherm: adiabatic gradient (usually 0.4-0.5 K/km) and potential temperature

- ✓ $T@410 \text{ km} = 1520 - 1600 \text{ }^{\circ}\text{C}$ (Katsura 2022)

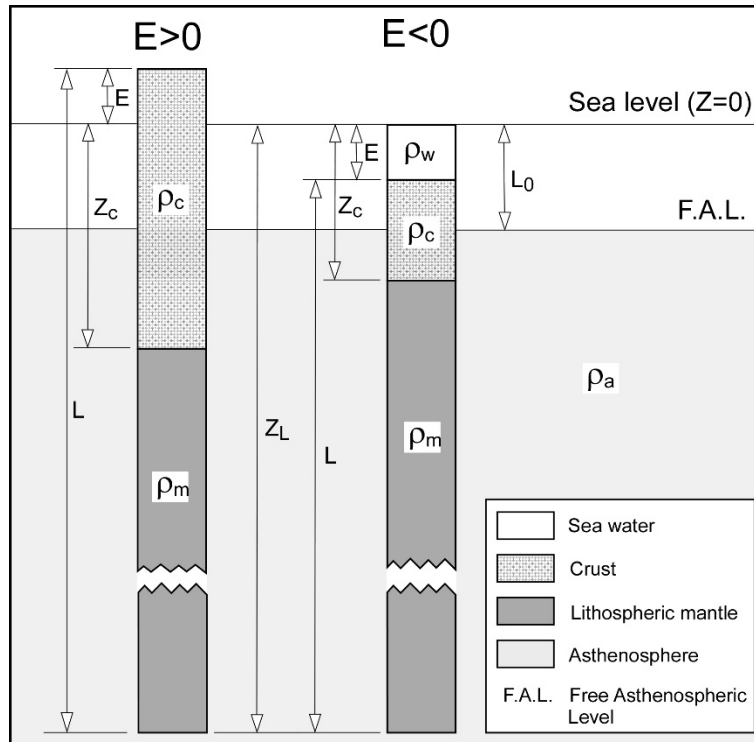


Surface heat Flow and lithospheric thickness



Isostasy

- ✓ **Lithospheric isostasy: (absolute) elevation as a measure of the bouyancy of the lithosphere**



$$\int_{LC} \Delta\rho(z) dz = 0$$

$$E = \frac{\rho_a - \rho_L}{\rho_a} \cdot L - L_0 \quad (E > 0)$$

$$E = \frac{\rho_a}{\rho_a - \rho_w} \cdot \left(\frac{\rho_a - \rho_L}{\rho_a} \cdot L - L_0 \right) \quad (E < 0)$$

$$\rho_L = \frac{(E + z_c)\rho_c + (z_L - z_c)\rho_m}{(E + z_L)}$$

(e.g. Lachenbruch & Morgan 1990)

- **Lithospheric mantle able to hold density contrasts over geological time scales...**

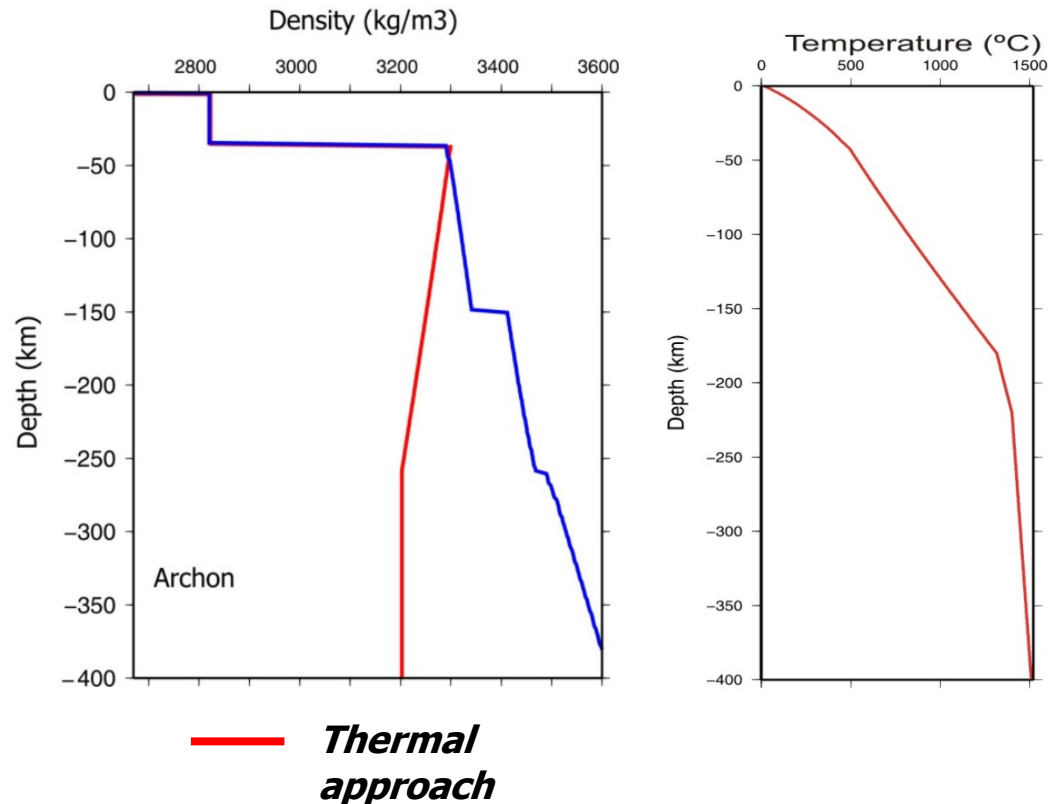
Local isostasy: average density of the lithosphere

Linear mantle density models (pressure effect neglected):

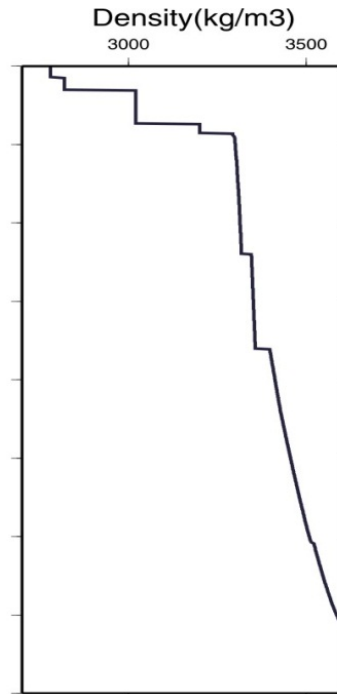
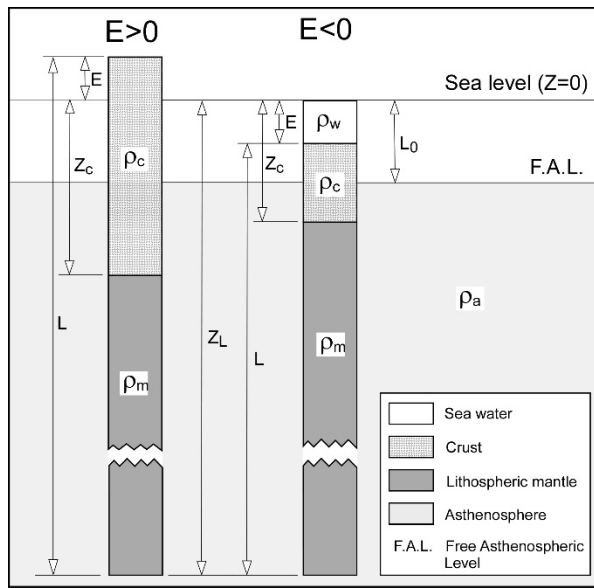
$$\rho_m(z) = \rho_a(1 + \alpha[T_a - T_m(z)])$$

$$\rho_m(z) = \rho_0(1 - \alpha[T_m(z)])$$

T_a Lithosphere-asthenosphere boundary temperature (1200-1315 C typically), α thermal expansion coefficient, ρ_a asthenospheric density (typically 3200 kg/m³), ρ_0 mantle density at the surface ($T=0$)



Local isostasy: average density of the lithosphere



$$\int_{LC} \Delta\rho(z) dz = 0$$

$$E = \frac{\rho_a - \rho_L}{\rho_a} \cdot L - L_0 \quad (E > 0)$$

$$E = \frac{\rho_a}{\rho_a - \rho_w} \cdot \left(\frac{\rho_a - \rho_L}{\rho_a} \cdot L - L_0 \right) \quad (E < 0)$$

$$\rho_L = \frac{(E + z_c)\rho_c + (z_L - z_c)\rho_m}{(E + z_L)}$$

Classical formulation of lithospheric isostasy (Lachenbruch & Morgan, 1990).

Includes variations in crustal and lithospheric thickness as well as crustal and mantle density.

A Mid Oceanic Ridge (MOR) is taken as the reference column (L_0)

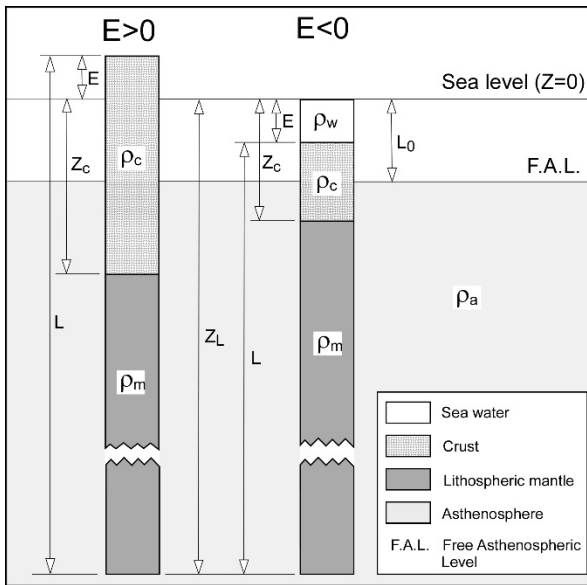


Local isostasy: average density of the lithosphere

In terms of pressure, P , at the compensation level (CL), for an arbitrary reference column with $E=0$:

$$P_{ref} = \int_0^{z_{cREF}} \rho_c dz + \int_{z_{cREF}}^{z_{LREF}} \rho_m(z) dz + \int_{z_{LREF}}^{CL} \rho_{msub}(z) dz$$

For any other column at the CL the pressure must be the same. If the average lithospheric density is $<$ reference lithospheric density the topography compensates the pressure deficit:



$$P_c = \int_0^{z_c} \rho_c dz + \int_{z_c}^{z_L} \rho_m(z) dz + \int_{z_L}^{CL} \rho_{msub}(z) dz + \int_0^{h_{cont}} \rho_c dz = P_{ref}$$

If the average lithospheric density is $>$ reference lithospheric density the bathymetry compensates the pressure excess:

$$P_c = \int_0^{z_c} \rho_c dz + \int_{z_c}^{z_L} \rho_m(z) dz + \int_{z_L}^{CL} \rho_{msub}(z) dz + \int_0^{h_{bathy}} (\rho_w - \rho_c) dz = P_{ref}$$

Mantle density-pressure coupling

The lithostatic pressure, P , at any depth depends on the weight of the lithospheric column above:

$$P = \rho g z$$

But in general $\rho = \rho(P)$, this coupling is solved numerically in an iterative scheme:

$$P_0(z) = P(z - \Delta z) + \rho(z - \Delta z) g \Delta z$$

$$\rho(z) = F(P_0(z)); \bar{\rho}_1 = \frac{\rho(z) + \rho(z - \Delta z)}{2}$$

$$P_1(z) = P(z - \Delta z) + \bar{\rho}_1 g \Delta z$$

$$\rho(z) = F(P_1(z)); \bar{\rho}_2 = \frac{\rho(z) + \rho(z - \Delta z)}{2}$$

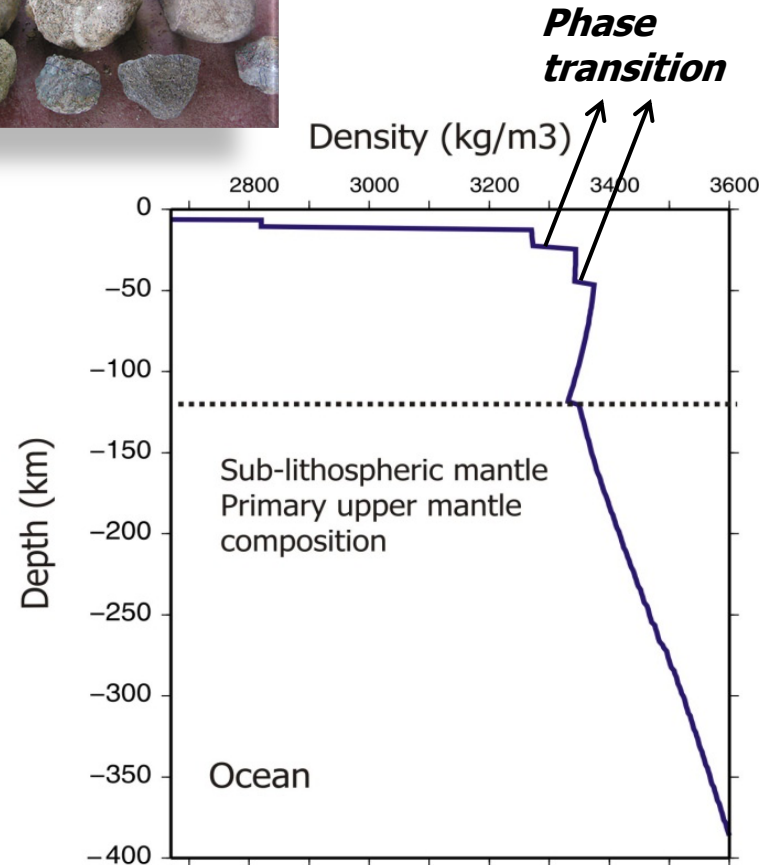
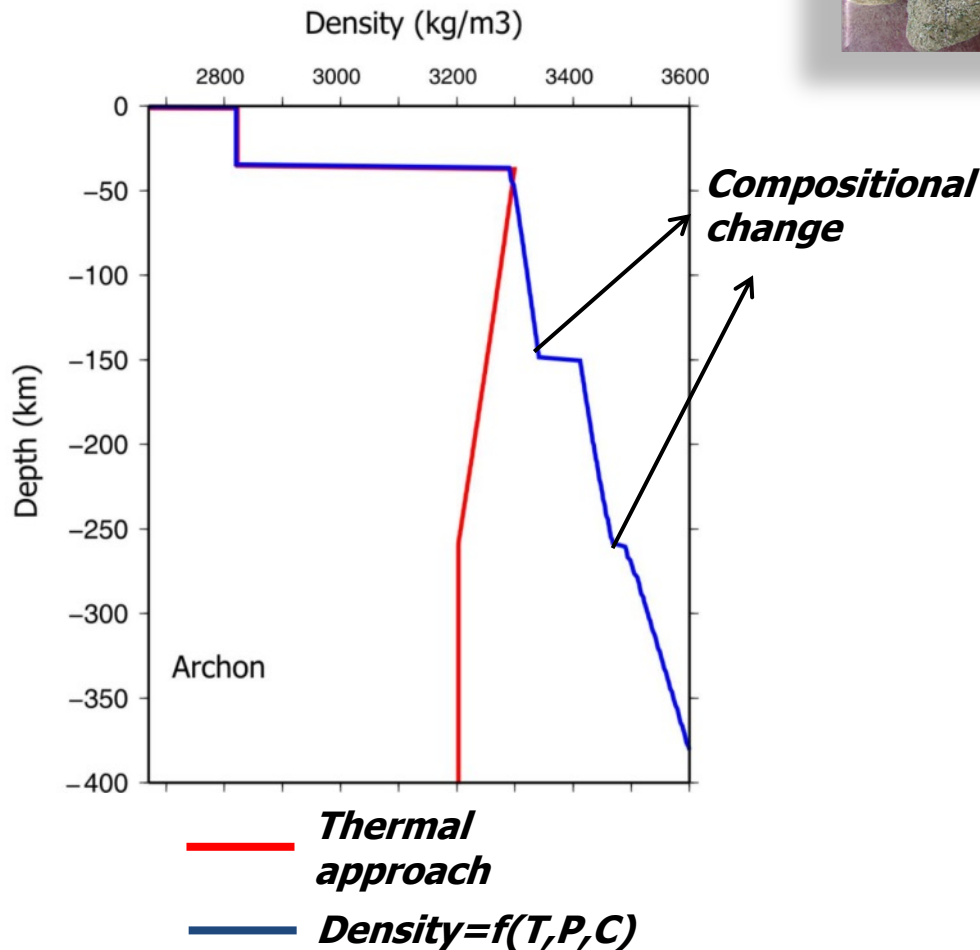
$$P_2(z) = P(z - \Delta z) + \bar{\rho}_2 g \Delta z$$

...

✓ Easy density dependence: Cold = dense = less buoyant

$$\rho_m(z) = \rho_a (1 + \alpha [T_a - T_m(z)])$$

Yes but, let's consider composition...



Summary of basic thermodynamic concepts

System: the region of interest, of sufficient size that average properties like temperature are well-defined; to be distinguished from the environment (i.e. the rest of the universe)

Isolated system: exchanges neither matter nor energy across its boundaries

Closed system: may exchange energy across boundaries, but not matter

Open system: may exchange matter and energy across boundaries

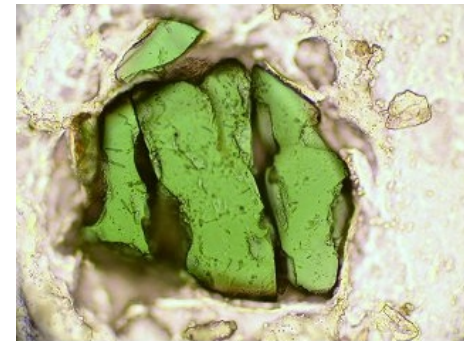
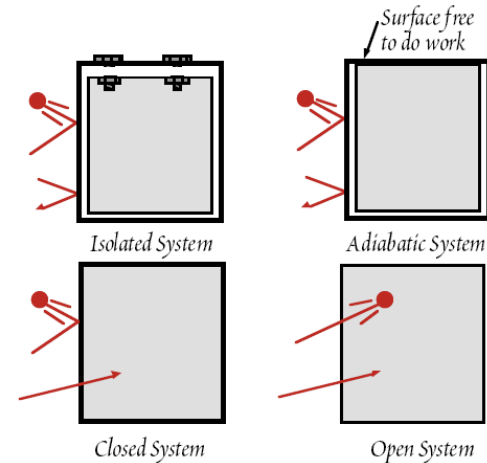
Phase: a physically homogeneous and mechanically separable part of the system, e.g. a vapor, liquid, or mineral. A system may be homogeneous (one phase) or heterogeneous (multiple phases). E.g. solid solution of Forsterite and Fayalite (Olivine end-member minerals).

Olivine Forsterite Mg_2SiO_4 \longrightarrow Fayalite Fe_2SiO_4

Plagioclase Albite $NaAlSi_3O_8$ \longrightarrow Anorthite $CaAl_2Si_2O_8$

Component: a chemical formula; a basis vector for expressing compositional variations in thermodynamic systems; e.g., H_2O , SiO_2 , Fe , $NaCl$. Must be independently variable, but we choose the minimum set to span all phases. Main oxides in the mantle NCFMAS system (sometimes also Cr_2O_3)

Phase vs system component (e.g. oxide).



Synthetic wadsleyite II

Summary of basic thermodynamic concepts

Gibbs free energy: is the energy available for non-PV work (such as chemical work)

$$G = H - TS \quad (13)$$

$$dG = VdP - SdT \quad (15)$$

Note that

$$(dG/dT)_P = -S$$

$$(dG/dP)_T = V$$

Since its independent variables are P and T , it is useful for equilibrium studies.

It also contains the entropy term which can be used as an indication of the direction in which spontaneous reactions will occur.

Note that if P and T remain constant through any spontaneous change in state, then $dG = 0$!!!!!!!!

- **Gibbs free energy is adequate for equilibrium studies because its independent variables are T and P , i.e. the ones we are usually interested in!**
- **Spontaneous reactions evolve to minimize the Gibbs free energy.**
- **At equilibrium, $dG = 0$ and $\Delta G = 0$. in other words, products and reactants are in equilibrium when their G are equal.**

Summary of basic thermodynamic concepts

$$\Delta G_{T',P'} = \Delta G_{T_{ref},P_{ref}} + \int_{P_{ref}}^{P'} \Delta V_r dP - \int_{T_{ref}}^{T'} \Delta S_r dT$$

$$\left(\frac{\partial \Delta G}{\partial T} \right)_P = -\Delta S$$

$$\left(\frac{\partial \Delta G}{\partial P} \right)_T = \Delta V$$

Solve this system iteratively for discrete ΔT and ΔP and find the point where $\Delta G = 0$

$$\Delta S(T) = \Delta S_{T_{ref}} + \int_{T_{ref}}^T \frac{\Delta C_p}{T} dT$$

How do we get the fundamental parameters?

Two main categories:

***Analysis of each phase individually (calorimetry, electrochemical)**

***Relate thermodynamic properties of minerals to each other (int. consist. dataset)**

The “solution” is a combination of calorimetric data and additional constraints such as reaction reversal brackets.

A thermodynamic dataset compatible with calorimetry and reaction reversals alike is called an *internally consistent thermodynamic dataset* (e.g. Holland and Powel 98, Stixrude 05, etc.)

Summary of basic petrological concepts

Ternary compositional plot for peridotites

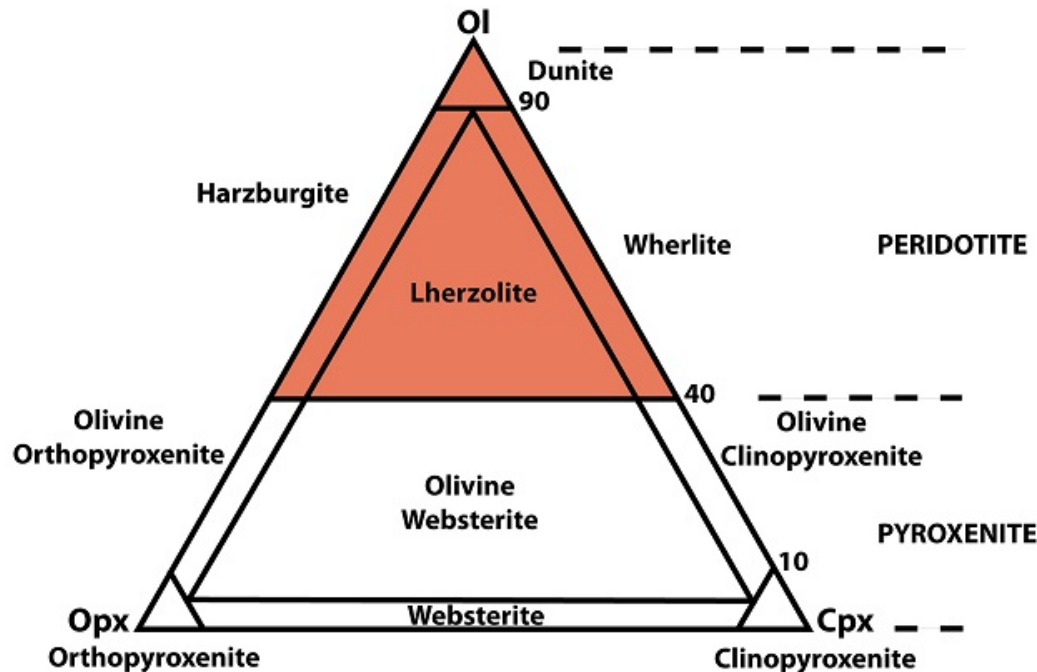


Table 15.2 | Mineralogy of Lherzolites

Mineral	Spinel Lherzolite		Garnet Lherzolite	
	Average (wt. pct.)	Range (vol. pct.)	Average (vol. pct.)	Range (vol. pct.)
Olivine	66.7	65-90	62.6	60-80
Orthopyroxene	23.7	5-20	30	20-40
Clinopyroxene	7.8	3-14	2	0-5
Spinel	1.7	0.2-3	—	—
Garnet	—	—	5	3-10
Phlogopite	—	—	0.4	0-0.5

Maaløe and Aoki (1977).

Peridotite as function of the stable mineral phases: Olivine (O), pyroxenes (cpx, opx), garnet(gnt) etc.

Summary of basic petrological concepts

Ternary compositional plot for peridotites

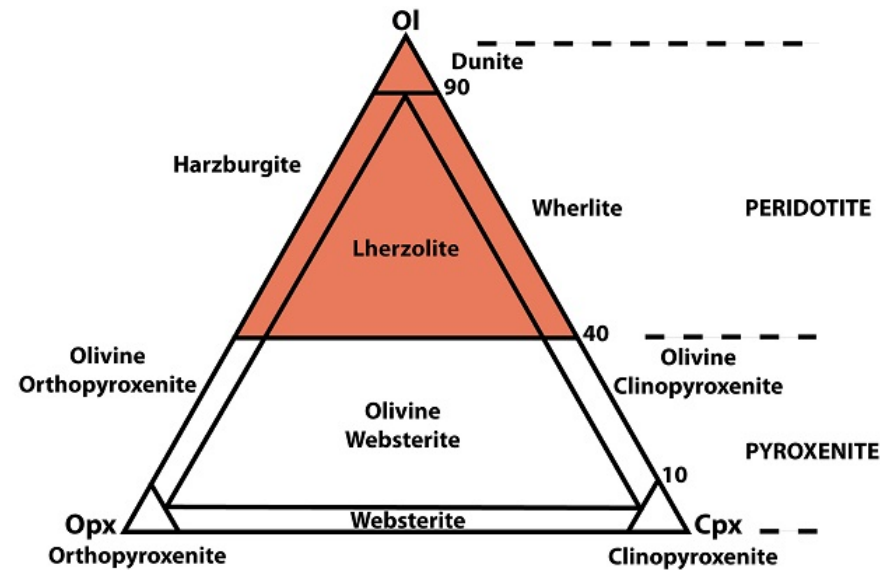


Table 15.3 | Compositions of peridotites and pyroxenites

Oxide	Lherzolites					Peridotites		
	Spinel (1)	(2)	Garnet (3)	Dunite (4)	Pyroxenite (5)	(6)	(7)	(8)
SiO ₂	44.15	44.40	44.90	41.20	48.60	44.14	46.36	42.1
Al ₂ O ₃	1.96	2.38	1.40	1.31	4.30	1.57	0.98	
FeO	8.28	8.31	7.89	11.0	10.0	8.31	6.56	7.10
MgO	42.25	42.06	42.60	43.44	19.10	43.87	44.58	48.3
CaO	2.08	1.34	0.82	0.80	13.60	1.40	0.92	
Na ₂ O	0.18	0.27	0.11	0.08	0.71	0.15	0.11	
K ₂ O	0.05	0.09	0.04	0.016	0.28	—	—	
MnO	0.12	0.17	0.11	0.15	0.18	0.11	0.11	
TiO ₂	0.07	0.13	0.06	0.06	0.83	0.13	0.05	
P ₂ O ₅	0.02	0.06	—	0.10	0.10	—	—	
NiO	0.27	0.31	0.26	—	—	—	—	
Cr ₂ O ₃	0.44	0.44	0.32	—	—	0.34	0.33	
H ₂ O	—	—	—	0.50	0.90	—	—	

Peridotite as function of the major oxide composition

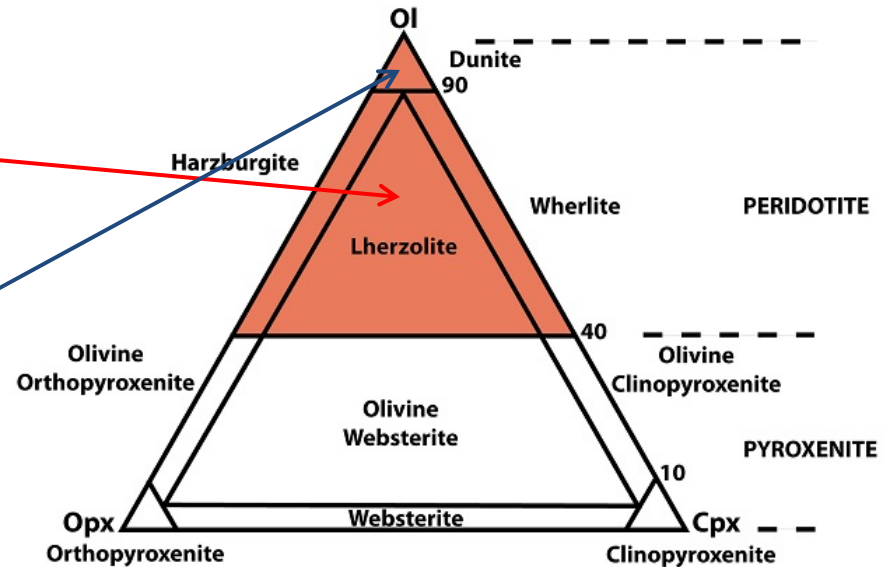
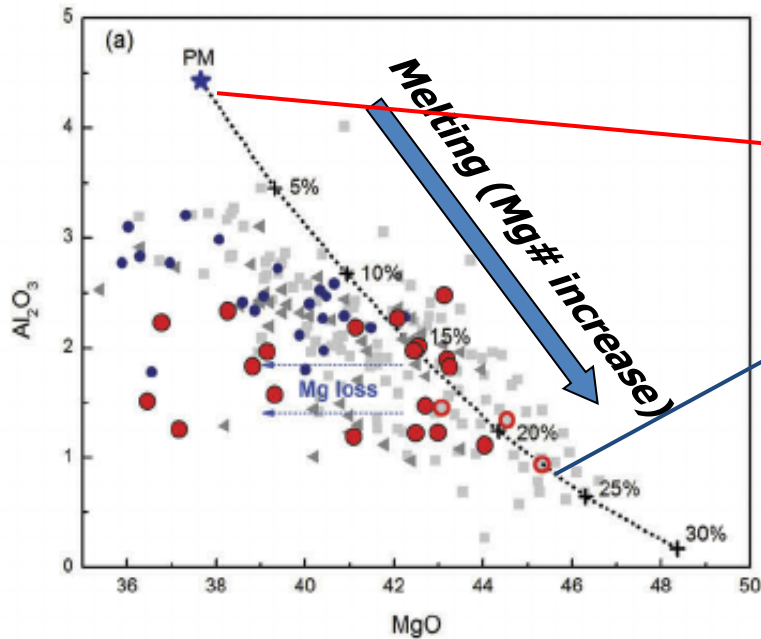
Summary of basic petrological concepts

Magnesium number: $Mg\# = MgO / (MgO + FeO)$

$Mg\#$ low \rightarrow fertile mantle (enriched in Al_2O_3 and CaO , depleted in MgO)

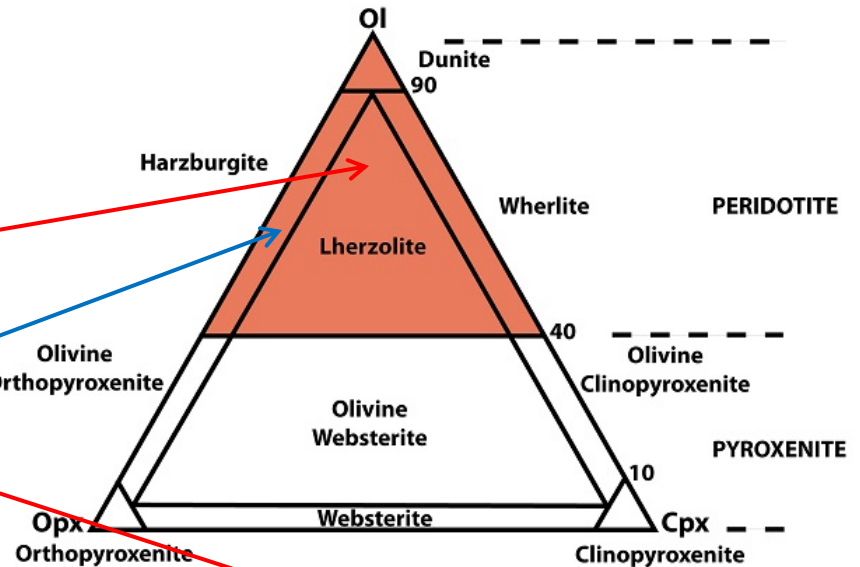
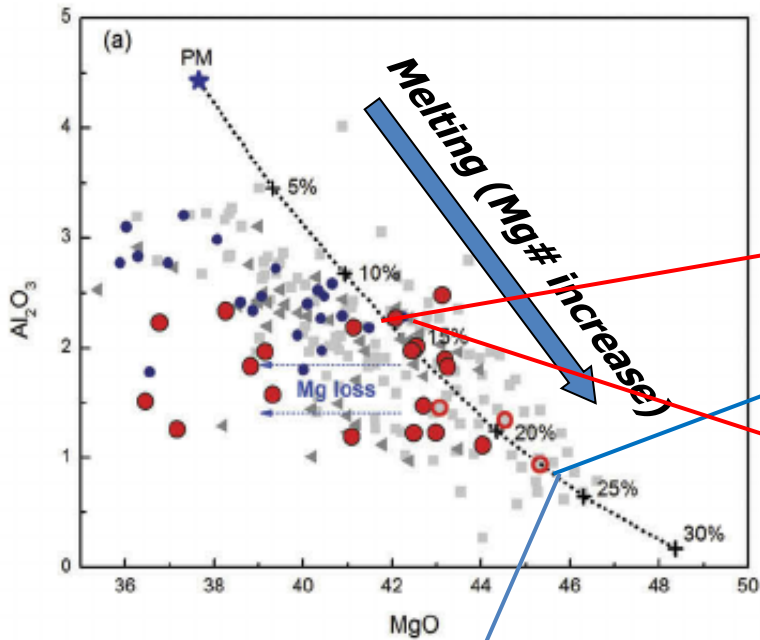
$Mg\#$ high \rightarrow refractory mantle (enriched in MgO , depleted in Al_2O_3 and CaO)

Melting trend



Summary of basic petrological concepts

Meting trend



	1) Av. Harz. Lanzarote (wt%) ^a	2) Av. HEXO Tenerife (wt%) ^b	3) Av. Harz. La Palma av. (wt%) ^c	4) Av. HLCO Tenerife (wt%) ^b	5) Av. Ocean floor peridot. (wt%) ^d	6) Av. Middle Atlas (wt%) ^e
SiO ₂	43.78	43.32	43.07	42.14	45.09	43.48
Al ₂ O ₃	0.7	0.61	0.53	0.73	2.33	2.38
FeO	7.79	8.04	8.43	8.8	8.4	8
MgO	46.1	45.31	45.19	44.14	41.23	42.6
CaO	0.6	0.81	0.68	1.68	1.32	2.83
Na ₂ O	0.1	0.14	0.17	0.18	0.23	0.24
Mg#	91.34	90.96	90.53	89.94	89.7	90.47



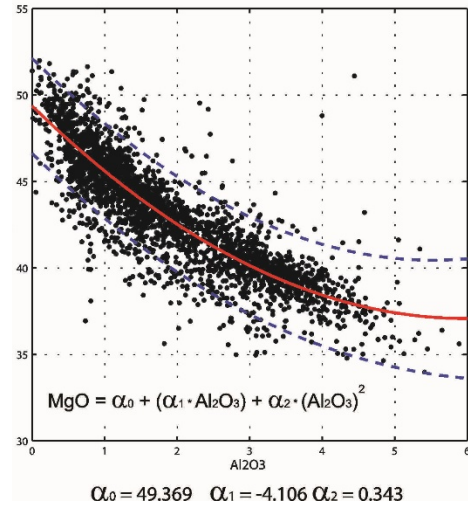
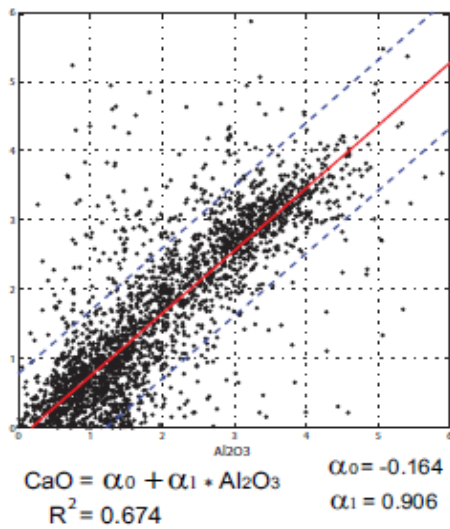
Mantle Depletion (partial meltina)

Mantle metasomatism (refertilization)

Compositional space: world petrological data bases

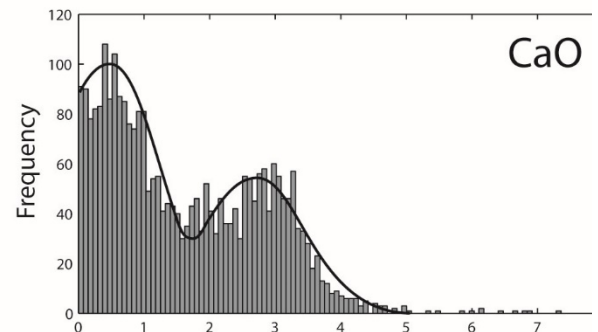
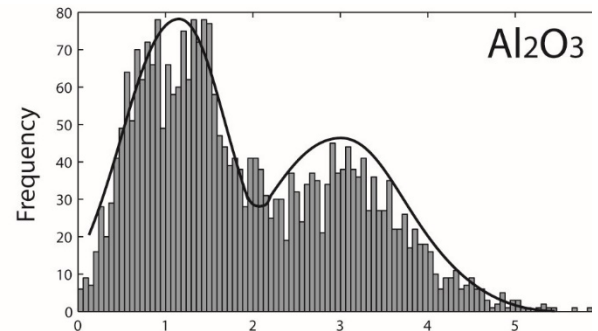
*Five major oxides (CFMAS (CaO-FeO-MgO-Al₂O₃-SiO₂)).

* A priori petrological data base (>2900 samples from xenoliths, perid. massifs and ophiolites)



Correlation between oxides regardless of tectonic age or facies.

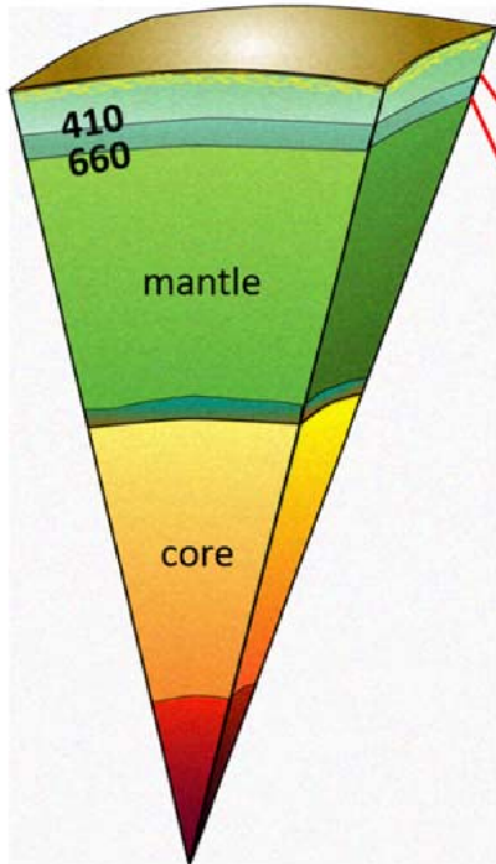
Al₂O₃ is strong compositional indicator, mainly through its control of modal garnet.



Possible bias in database (e.g. double peaks) due to sampling

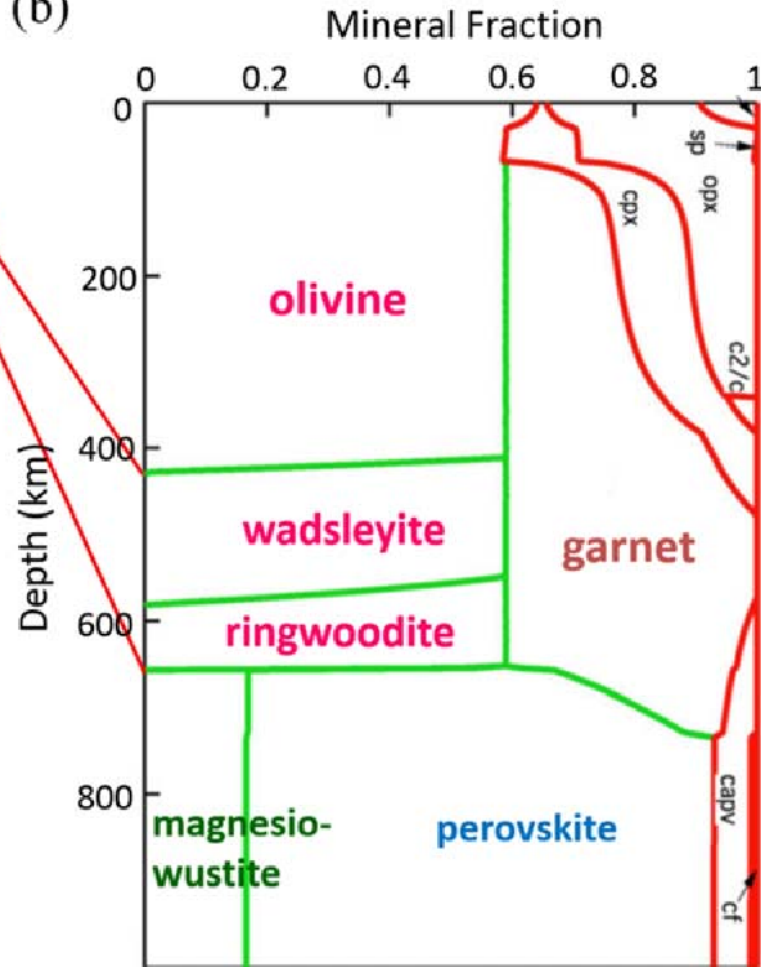
Summary of basic petrological concepts

(a)



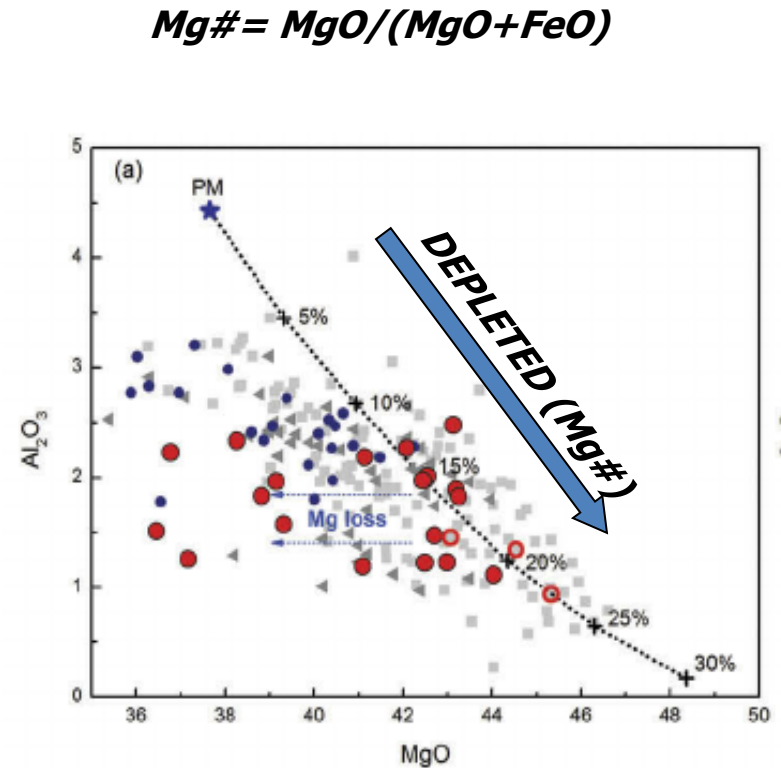
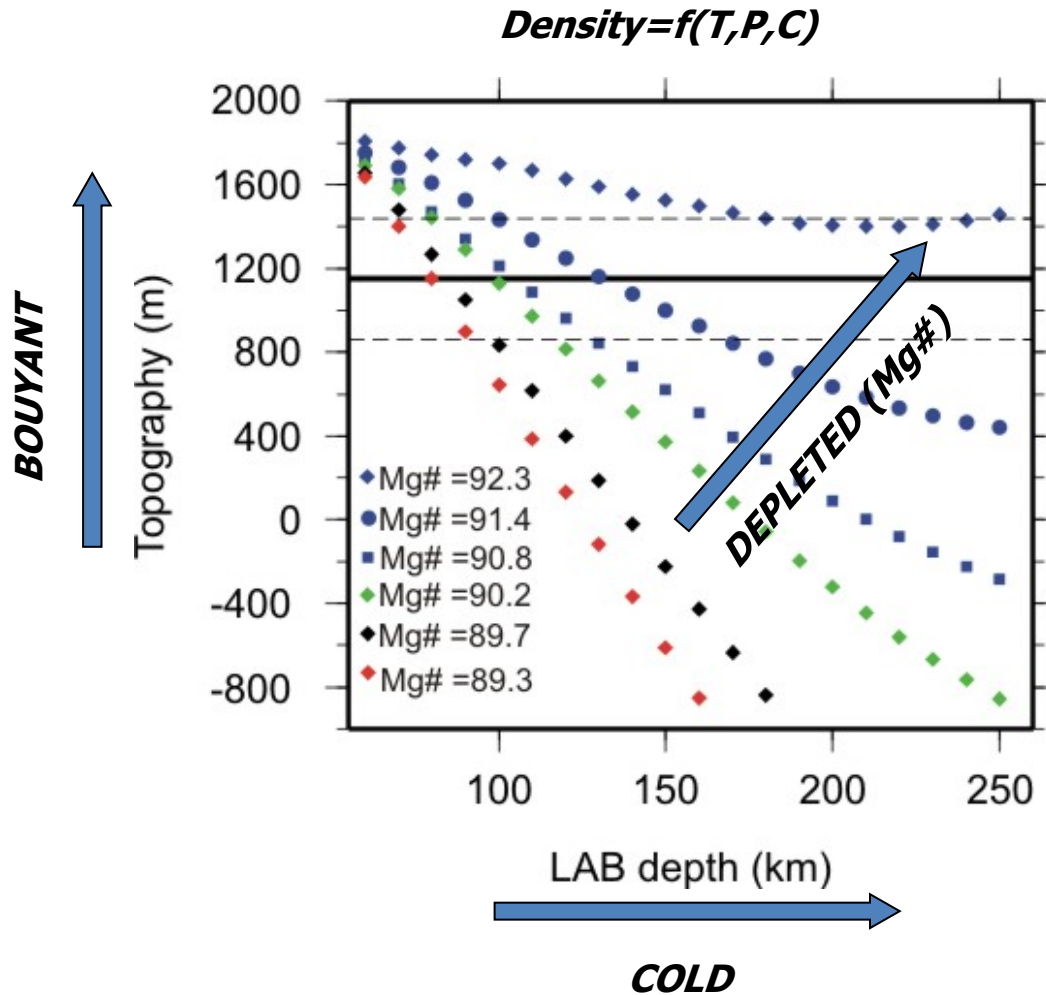
(From Ed Garnero's webpage)

(b)



(Modified from Xu et al., 2008)

Summary of basic petrological concepts



➤ **Mantle density is anti-correlated with Mg#...**

Summary of basic petrological concepts

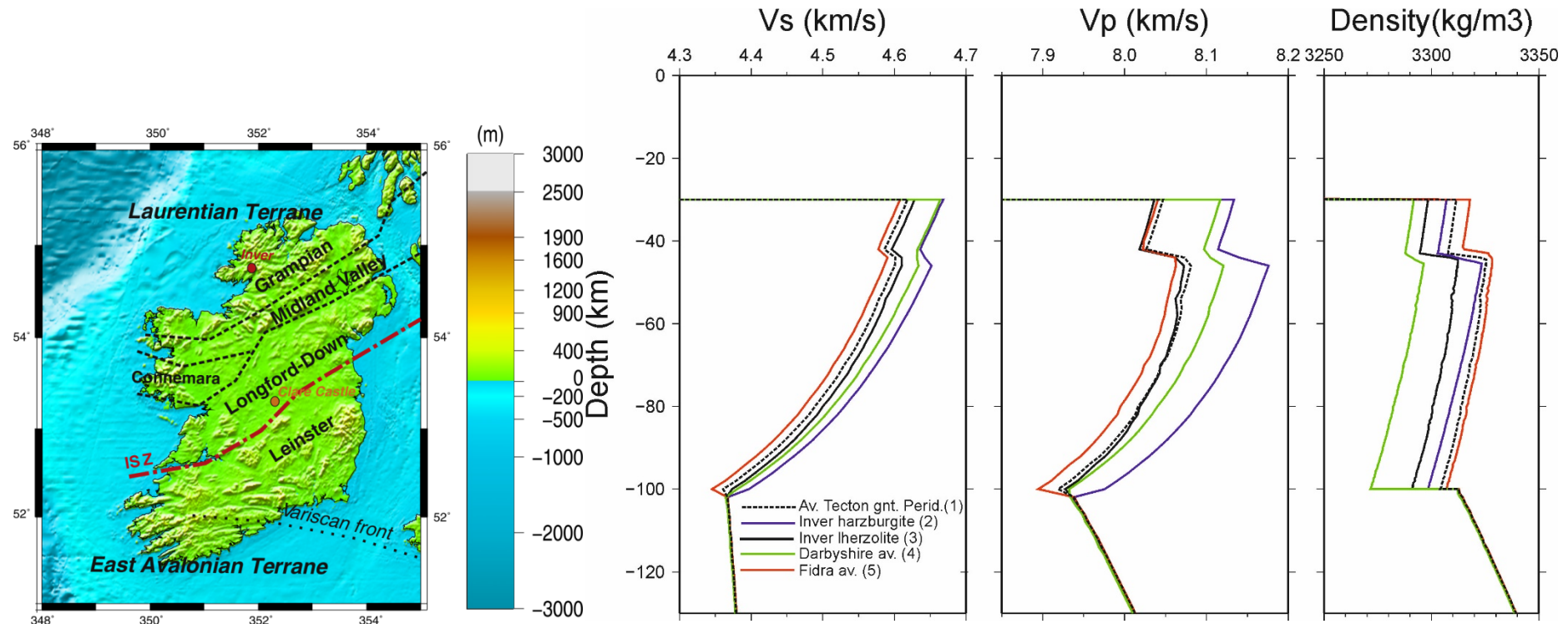


Table 1
Bulk mantle compositions used in this work from xenolith suites and peridotite massifs.

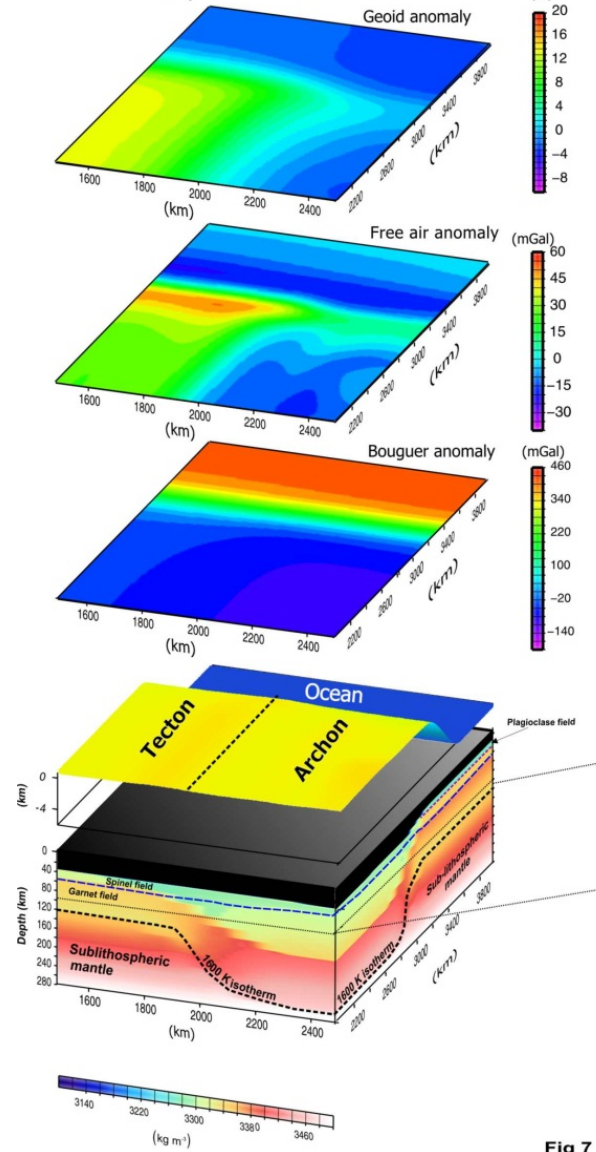
	1) Av. tecton gnt. perid. (wt.%) ^a	2) Harz. inver (wt.%) ^b	3) lherz. inver (wt.%) ^b	4) Derbyshire av. (wt.%) ^c	5) Fidra av. (wt.%) ^d	6) PUM M&S95 (wt.%) ^e
SiO ₂	45	41.7	45.84	43.4	44.31	45
TiO ₂	0.16	-	-	0.02	0.15	0.201
Al ₂ O ₃	3.9	2.65	3.92	2	3.5	4.45
Cr ₂ O ₃	0.41	-	-	0.51	-	0.384
FeO	8.1	8.32	7.19	7.4	8.6	8.05
MnO	0.07	-	-	0.22	0.14	0.135
MgO	38.7	44.86	38.05	44.5	38.5	37.8
CaO	3.2	0.77	2.72	1.5	3.3	3.55
Na ₂ O	0.28	0.05	0.21	0.08	0.3	0.36
NiO	0.24	-	-	0.32	-	-
Total	100.06	-	-	99.95	99.8	99.93
Mg#	89.5	90.58	90.42	91.47	87.73	89.3

➤ Mantle density is a **complex** function of **T** and **C** (no shortcuts...)

Density=f(T,P,C)

Same geotherm, different chemical layering

Thermal approach



➤ **Mantle has a strong impact in lithospheric density (buoyancy)!!**

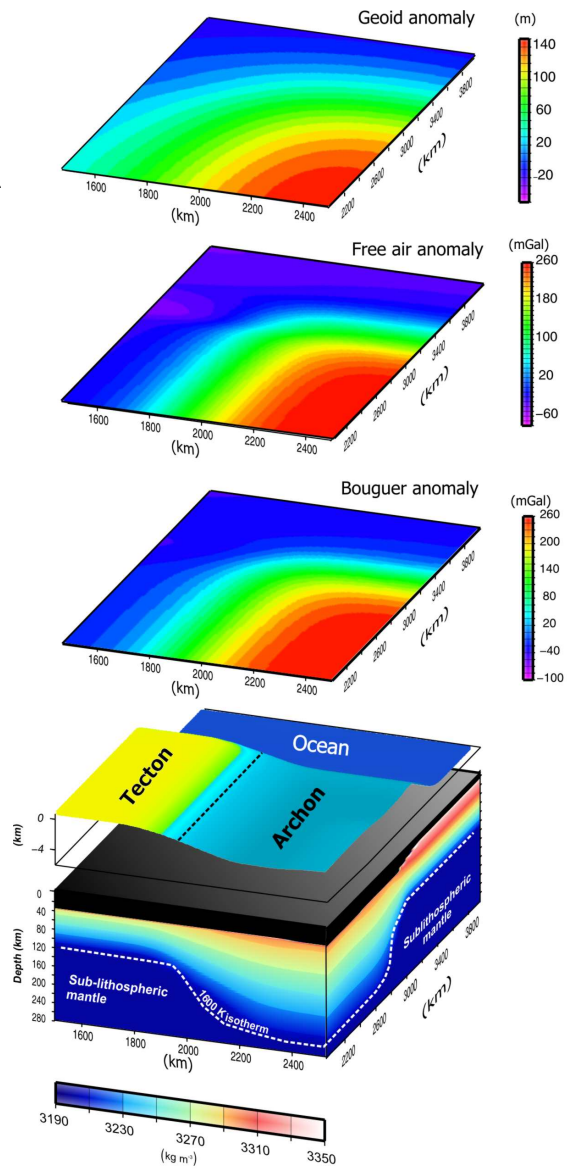
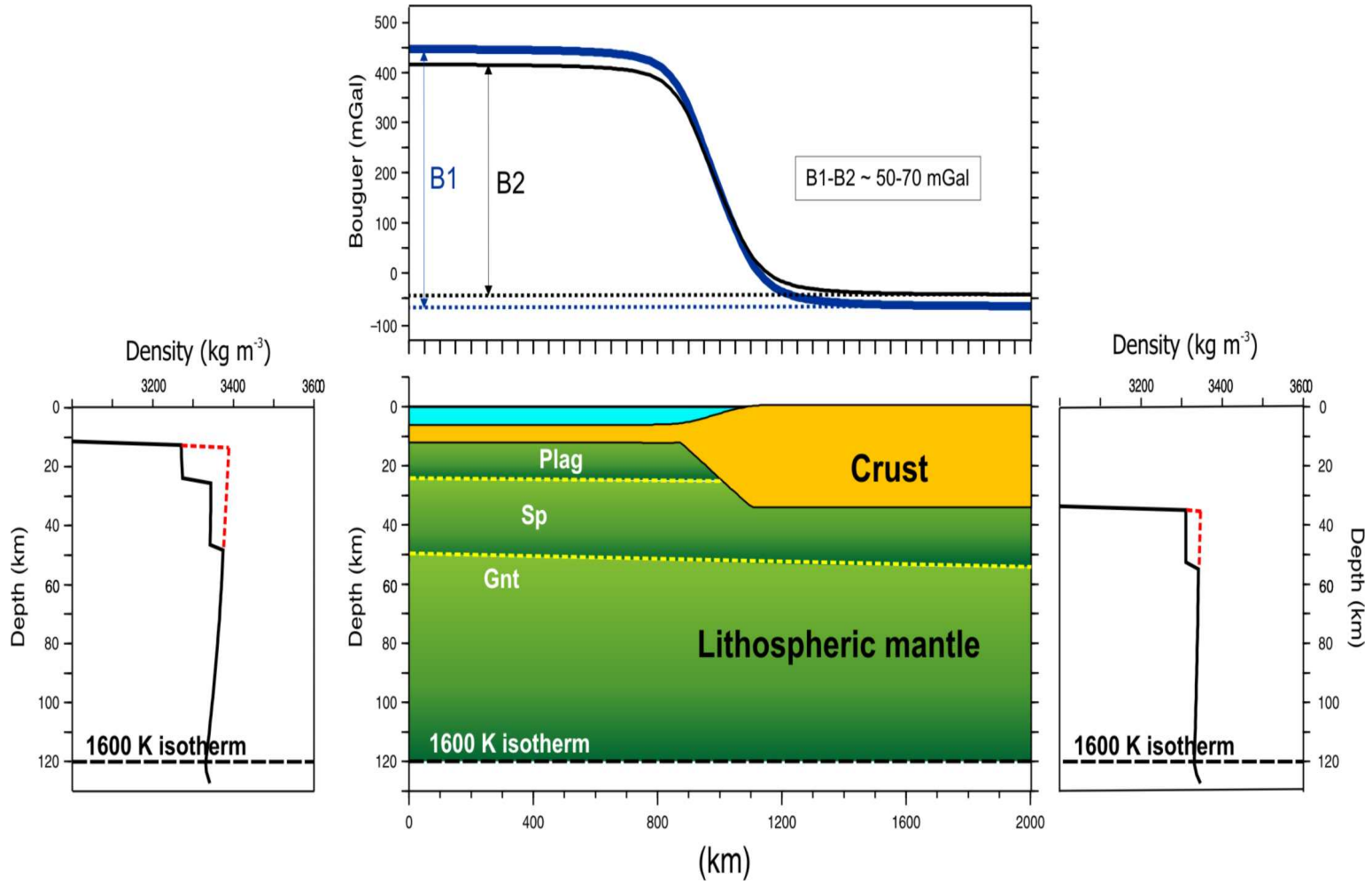


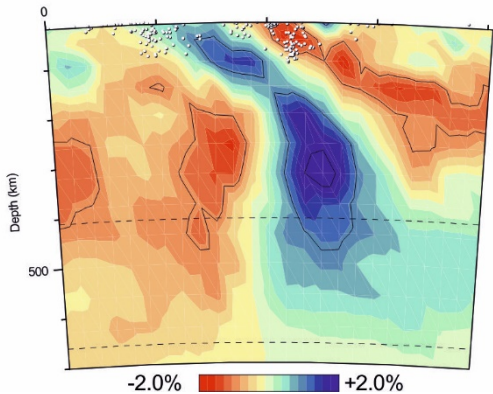
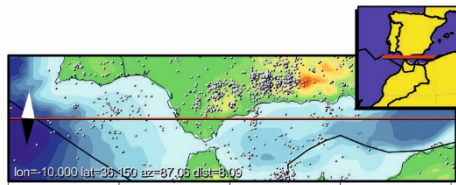
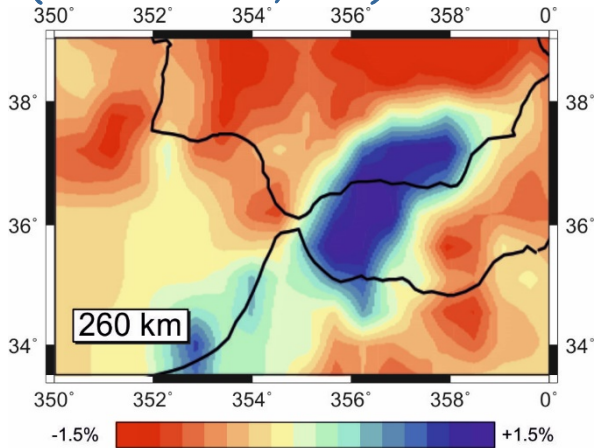
Fig 7

Upper mantle phase transitions

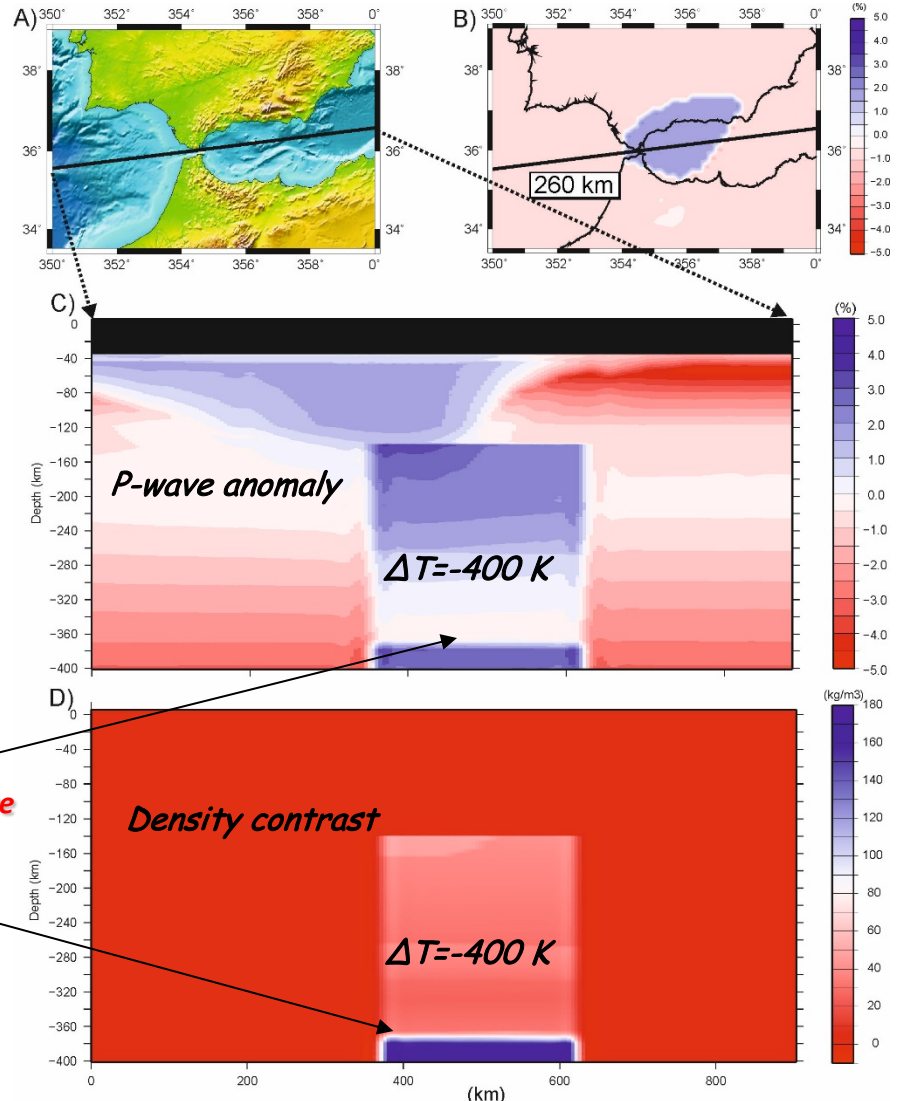
Differences in synthetic Bouguer anomaly due to shallow phase transitions (Al-bearing minerals)



*P-wave anomaly seismic tomography model
(Villaseñor et al., 2003)*



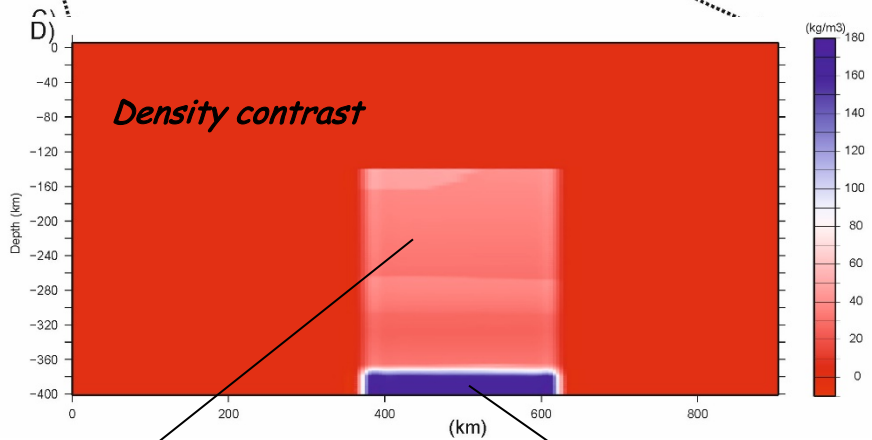
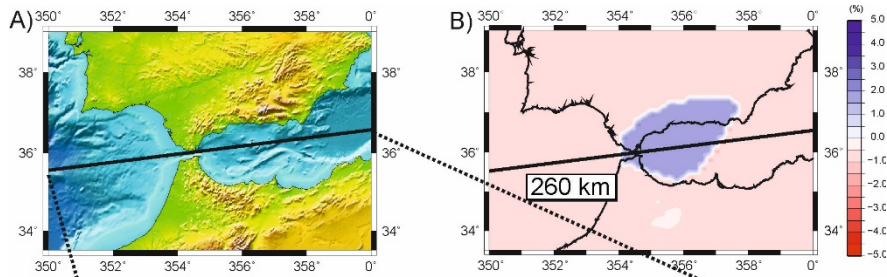
Simplified slab with $\Delta T = -400$ K with respect to ambient mantle based on geodynamic modelling of the Alboran Sea since upper Oligocene (Fullea et al. 2015)



*olivine \rightarrow wadsleyite
mineral phase
transition*

Simplified slab with $\Delta T = -400\text{ K}$ with respect to ambient mantle based on geodynamic modelling of the Alboran Sea since upper Oligocene (Fullea et al. 2015)

Sublithospheric thermal anomaly effect on gravity field

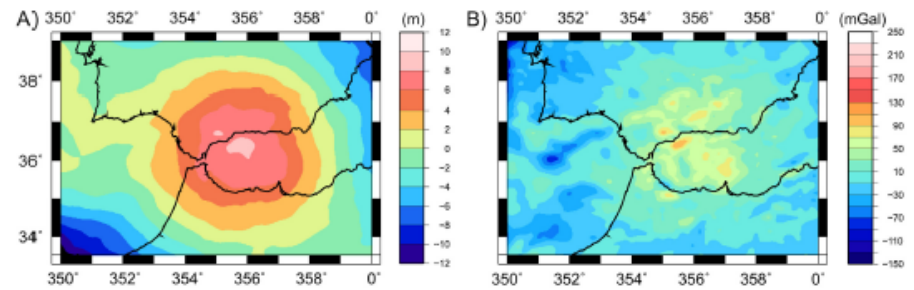


thermal
 $\Delta\rho = +25-40\text{ kg/m}^3$

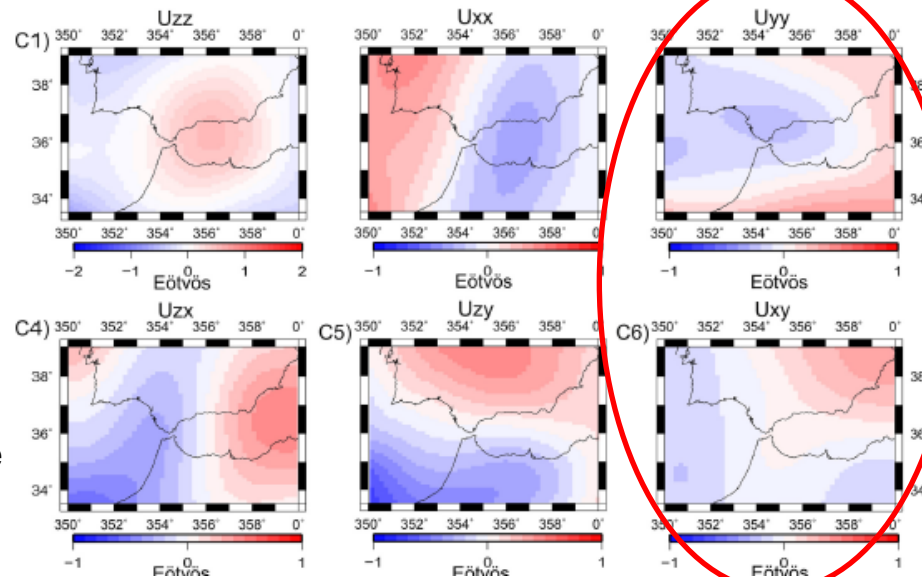
Thermal+phase change
 $\Delta\rho = +160\text{ kg/m}^3$

Geoid anomaly

Bouguer anomaly



Gravity gradients @ 255 km

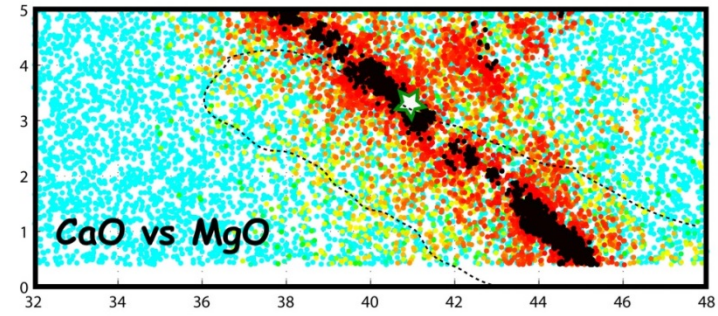
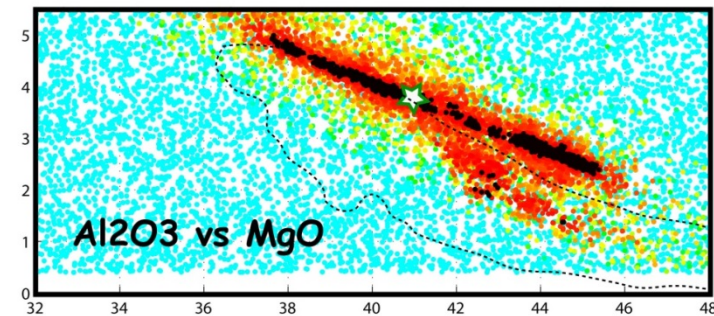
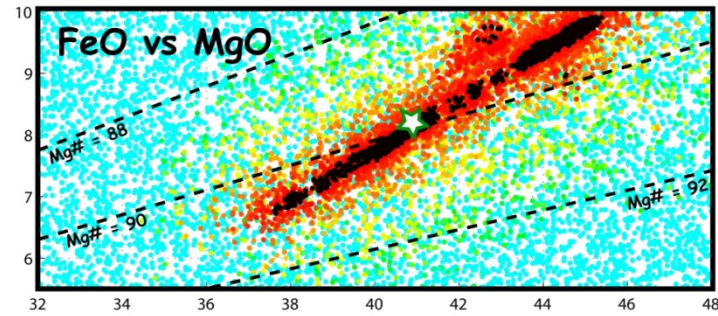
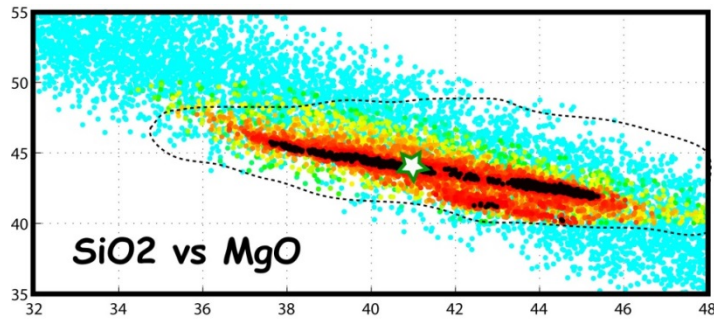


*Weaker effect in xy
and yy in components*

Complex parameter space

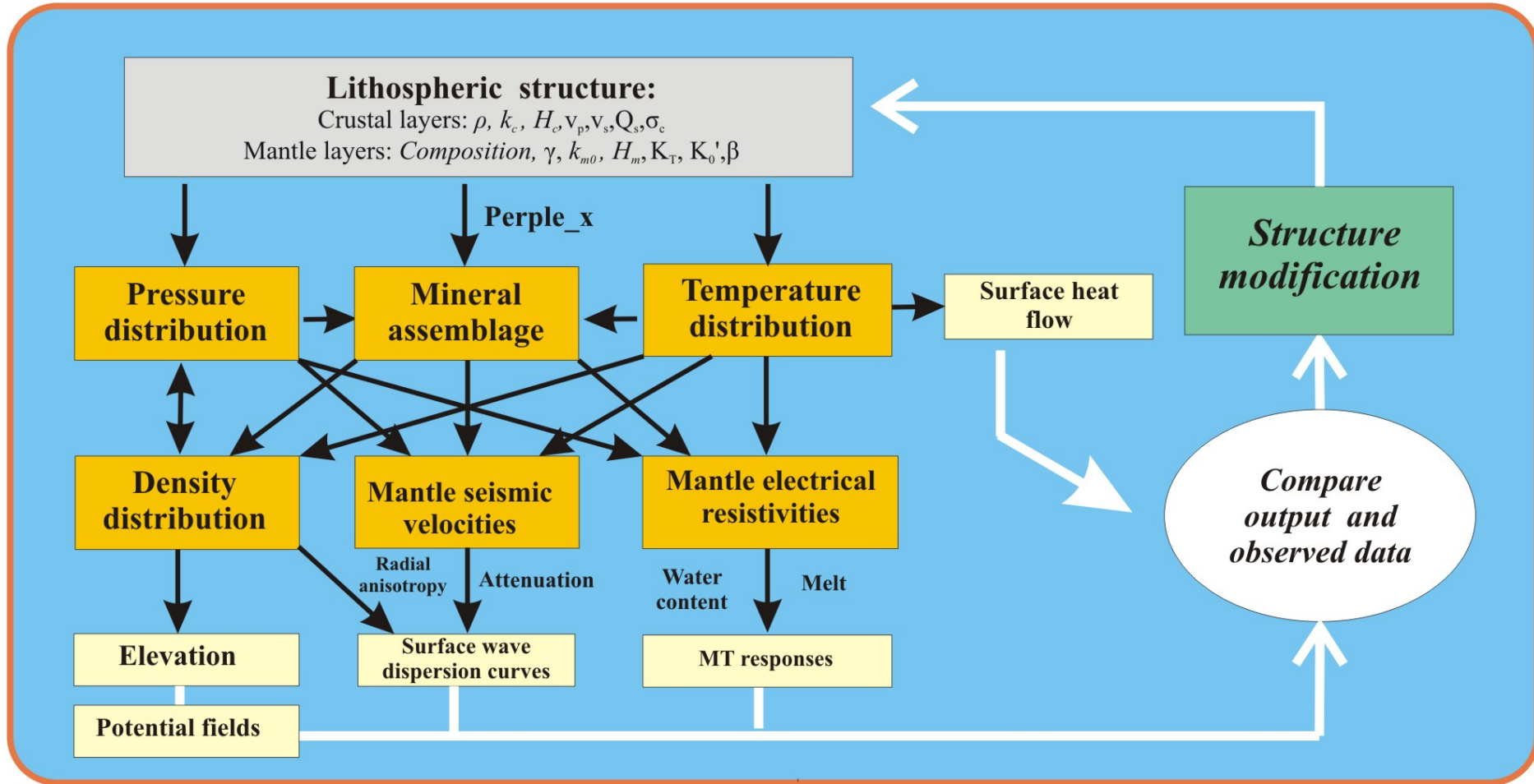
- * Trade-offs between Temperature and Composition
- * T has a greater effect than C in most of the observables
- * Non uniqueness of compositional field (worse in the lithosphere than in the sublithosphere)

$$\sigma(\mathbf{m}) = k\rho(\mathbf{m})L(\mathbf{m}) \quad L(\mathbf{m}) \propto \exp \left\{ -\frac{1}{2} [\mathbf{g}(\mathbf{m}) - \mathbf{d}_{\text{obs}}]^T C_D^{-1} [\mathbf{g}(\mathbf{m}) - \mathbf{d}_{\text{obs}}] \right\}$$



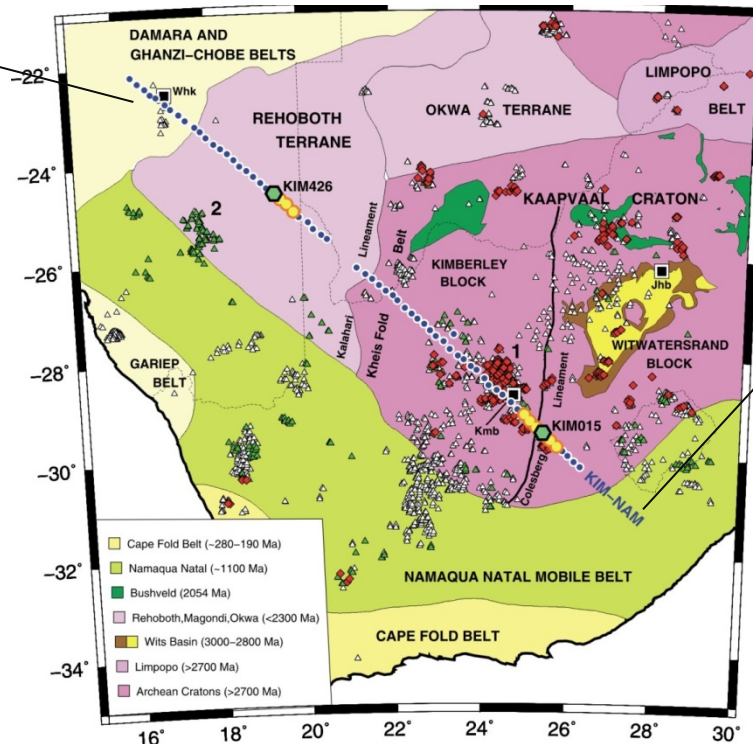
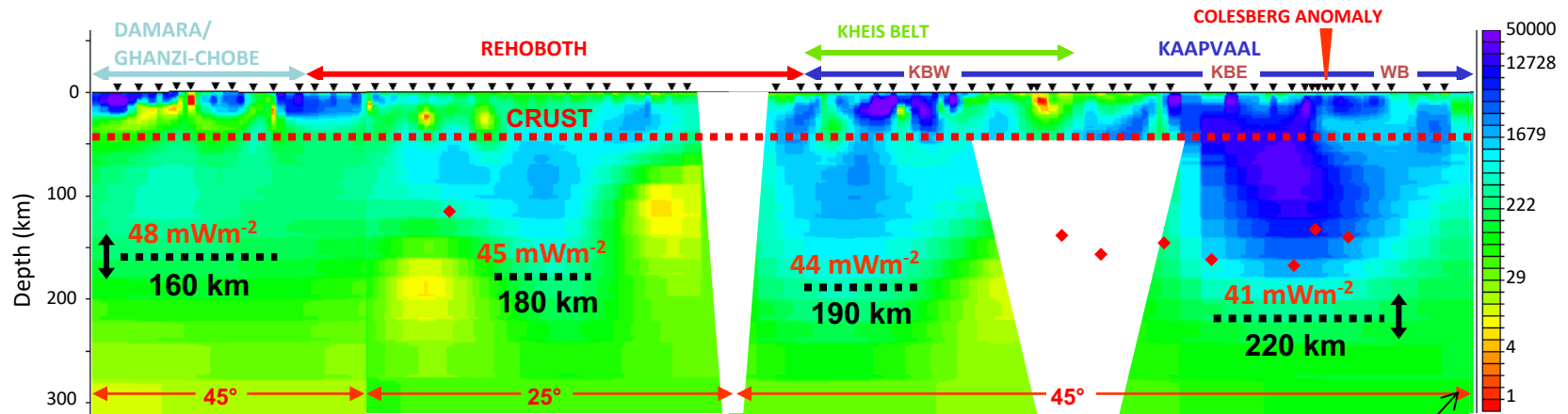
combined residual Vp, Vs, ρ

Integrated forward modelling: work flow



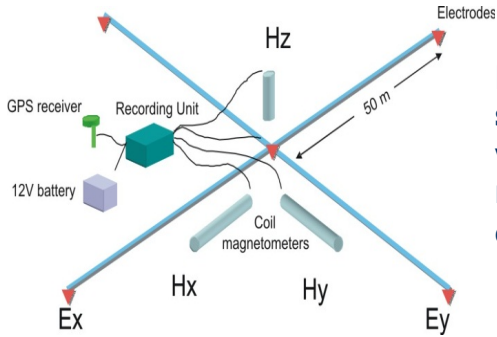
***Integrated modelling Magnetotelluric data
(Kaapvaal craton)***

Kaapvaal craton (S. Africa): 2D magnetotelluric (MT) model



SAMTEX (e.g., Muller et al., 2009, Evans et al., 2011)

Magnetotellurics (MT)



**MT site:
simultaneous
variations of
magnetic and
electric fields**

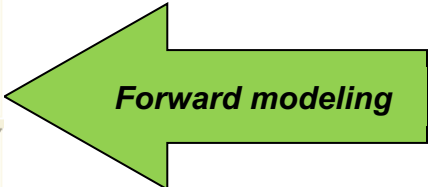
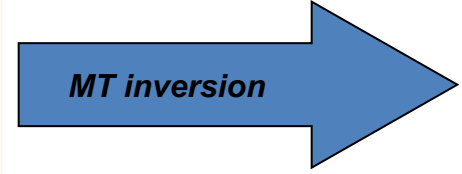
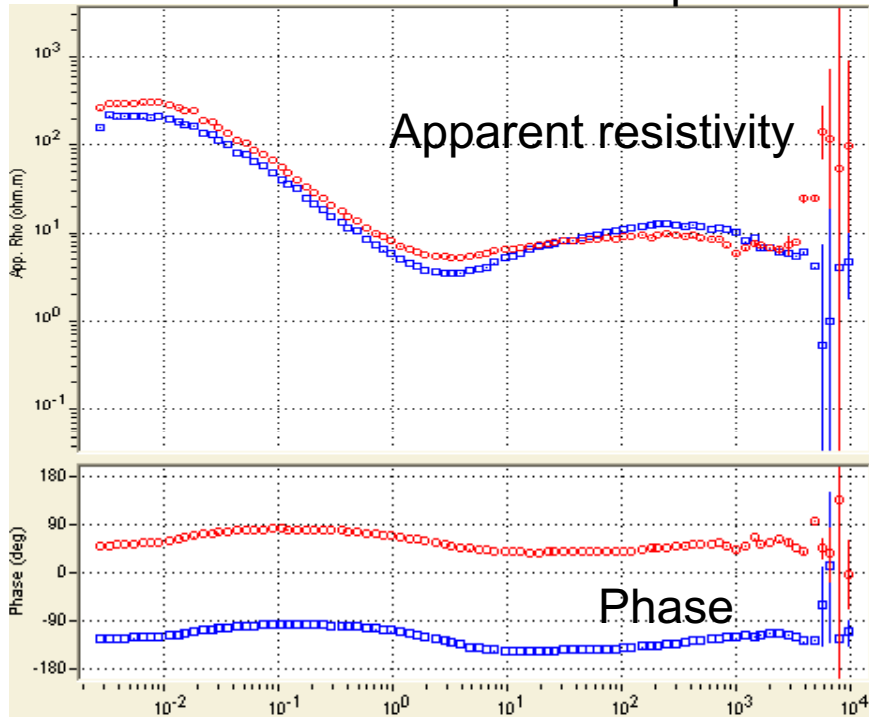
Apparent resistivity

$$\rho_{a,xy}(\omega) = \frac{1}{\omega\mu} \left| \frac{E_x(\omega)}{H_y(\omega)} \right|^2$$

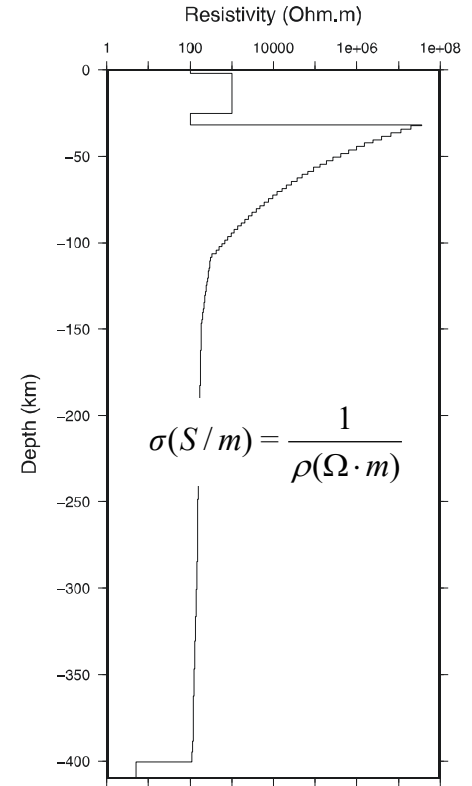
Phase

$$\varphi_{xy}(\omega) = \tan^{-1}(E_x(\omega)/H_y(\omega))$$

Processed MT station response



Resistivity (1/Conductivity)

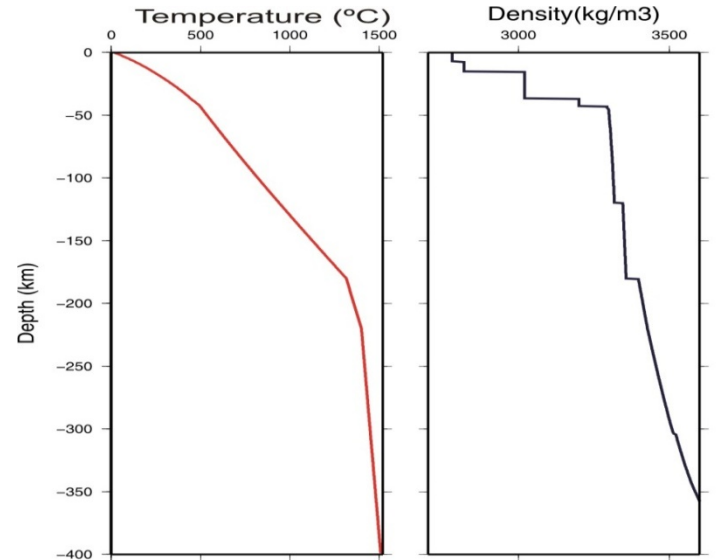
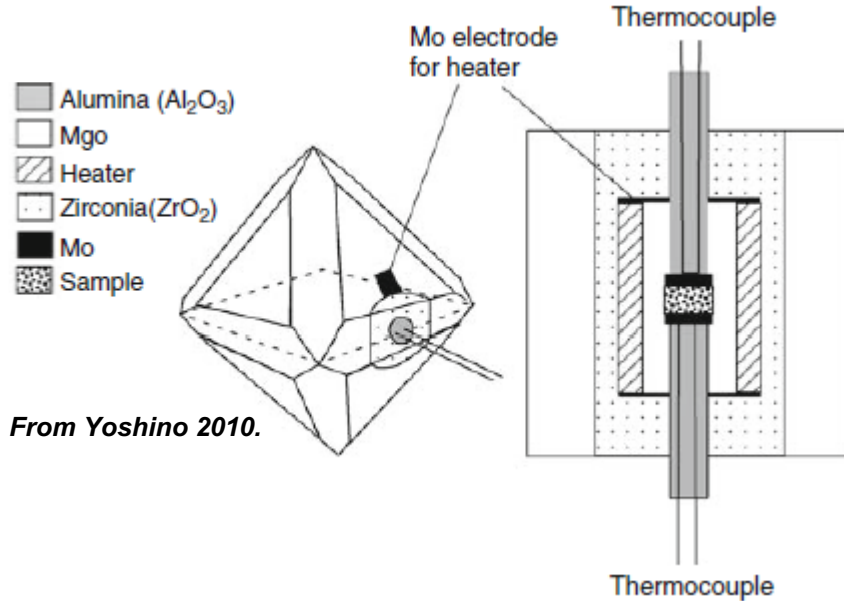


**Mineral
physics+lab
experiments**

**Temperature, pressure
and composition**

Electrical conductivity: lab experiments and mineral physics

Experimental measurements of conductivity in single crystals or mineral aggregates



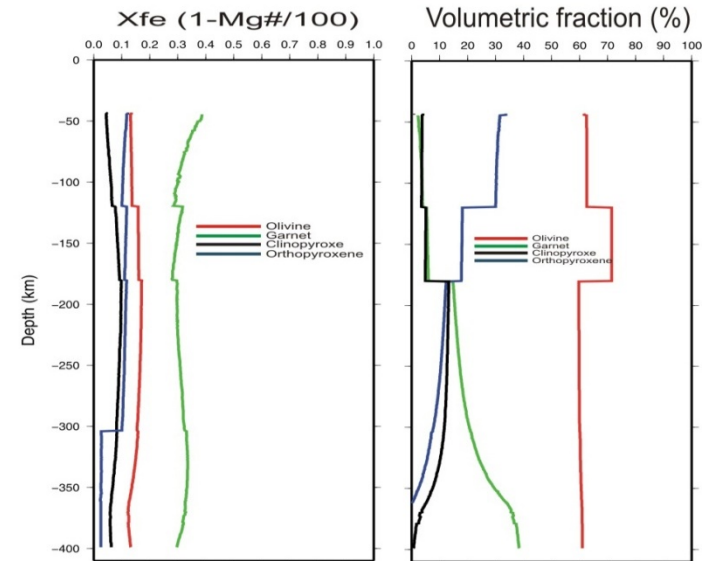
The electrical conductivity of the mantle minerals is typically of the form:

$$\sigma = \underbrace{\sigma_0 \exp\left(\frac{-\Delta H(X_{Fe}, P)}{k_B T}\right)}_{\text{small polaron}} + \underbrace{f(C_w) \exp\left(\frac{-\Delta H_{wet}(C_w)}{k_B T}\right)}_{\text{Proton conduction}} + \underbrace{\sigma_{0i} \exp\left(\frac{-\Delta H_i}{k_B T}\right)}_{\text{Ionic conduction}}$$

small polaron
(electron hopping
between ferric
Fe³⁺ and ferrous
Fe²⁺ ions) at
T < 1300 °C

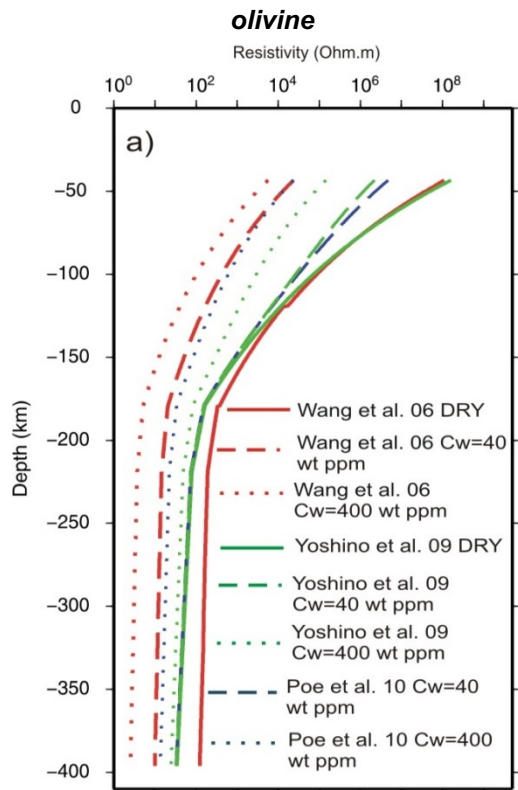
Proton
conduction
(H⁺ bound
to
structural
O atoms)

Ionic
conduction
(Mg
vacancies)
T > 1300 °C



Electrical conductivity: the water problem

Laboratory uncertainties/discrepancies

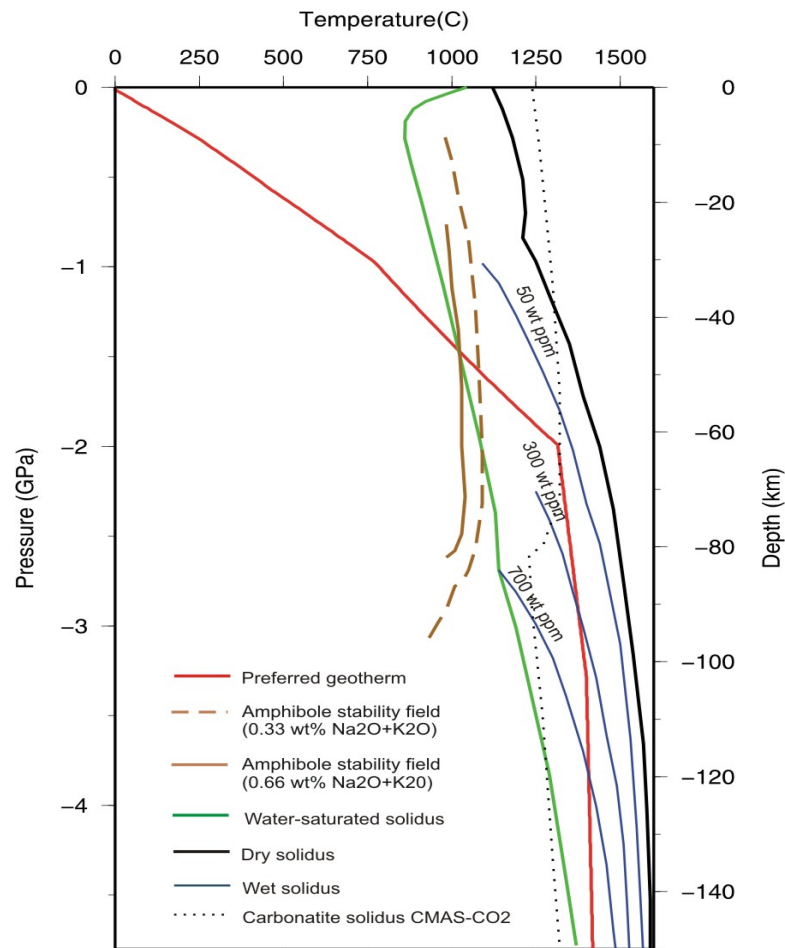


For olivine there are two models for proton conduction based on lab studies:

$$\sigma_P = \sigma_{0p} C_w \exp\left(\frac{-\left(\Delta H_0 - \alpha C_w^{1/3}\right)}{k_B T}\right) \rightarrow \text{e.g. Yoshino et al., 09; Manthilake et al., 09;}$$

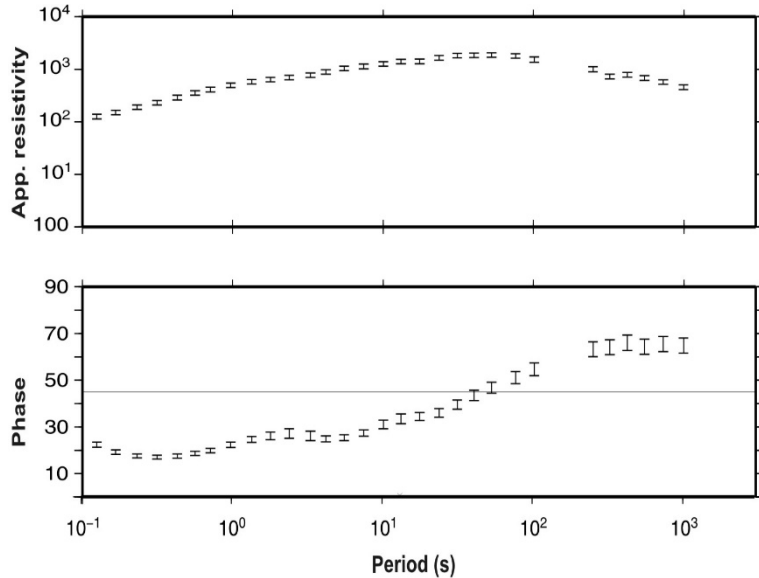
$$\sigma_P = A C_w^r \exp\left(\frac{-\Delta H_{wet}}{k_B T}\right) \rightarrow \text{Poe et al., 10 e.g. Wang et al., 06; Dai and Karato 09}$$

Peridotite solidus

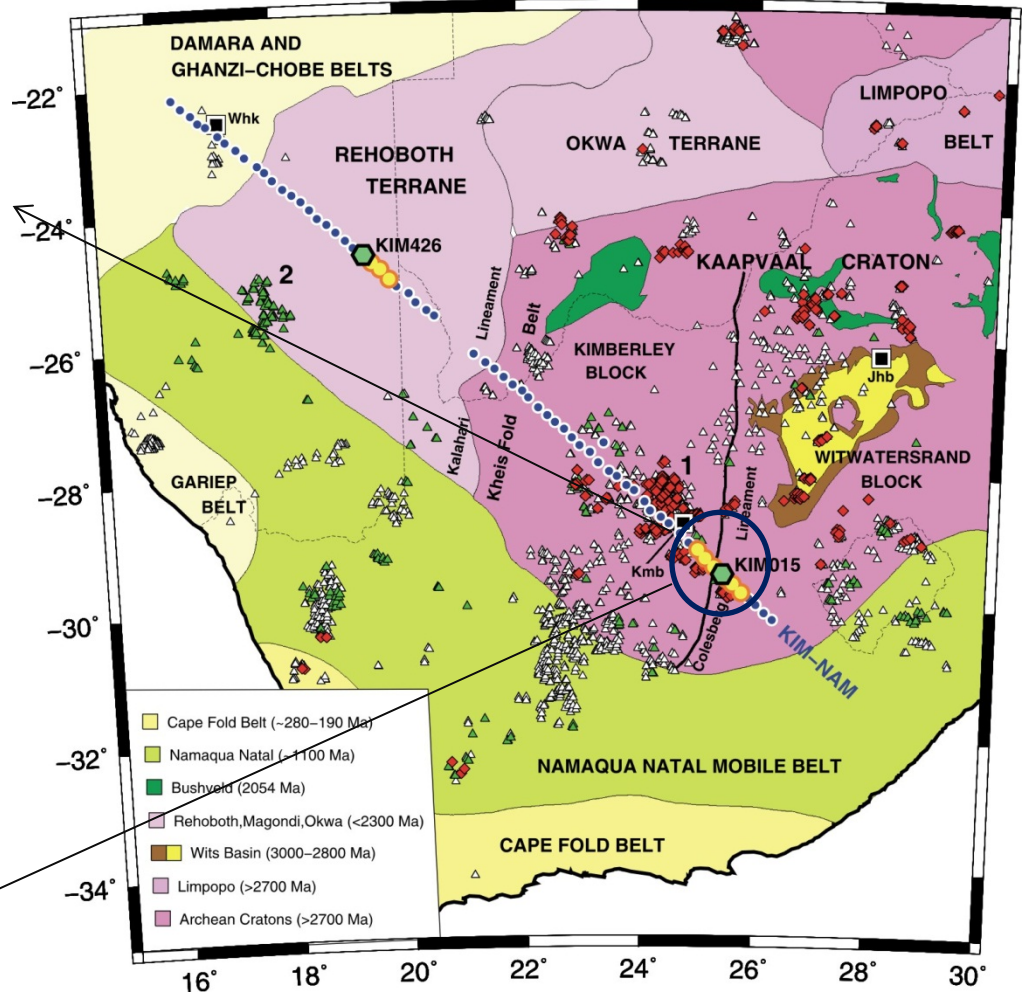


From Asimow et al. (2004)

observed MT responses



SAMTEX (e. g., Jones et al., 2009; Muller et al., 2009, Evans et al., 2011, Miensoopust et al., 2001)



The error bars reflect: the maximum of the data processing errors + Groom and Bailey decomposition model errors + departure from a 1D (differences between the TM and TE modes)

Elevation=1.34 km

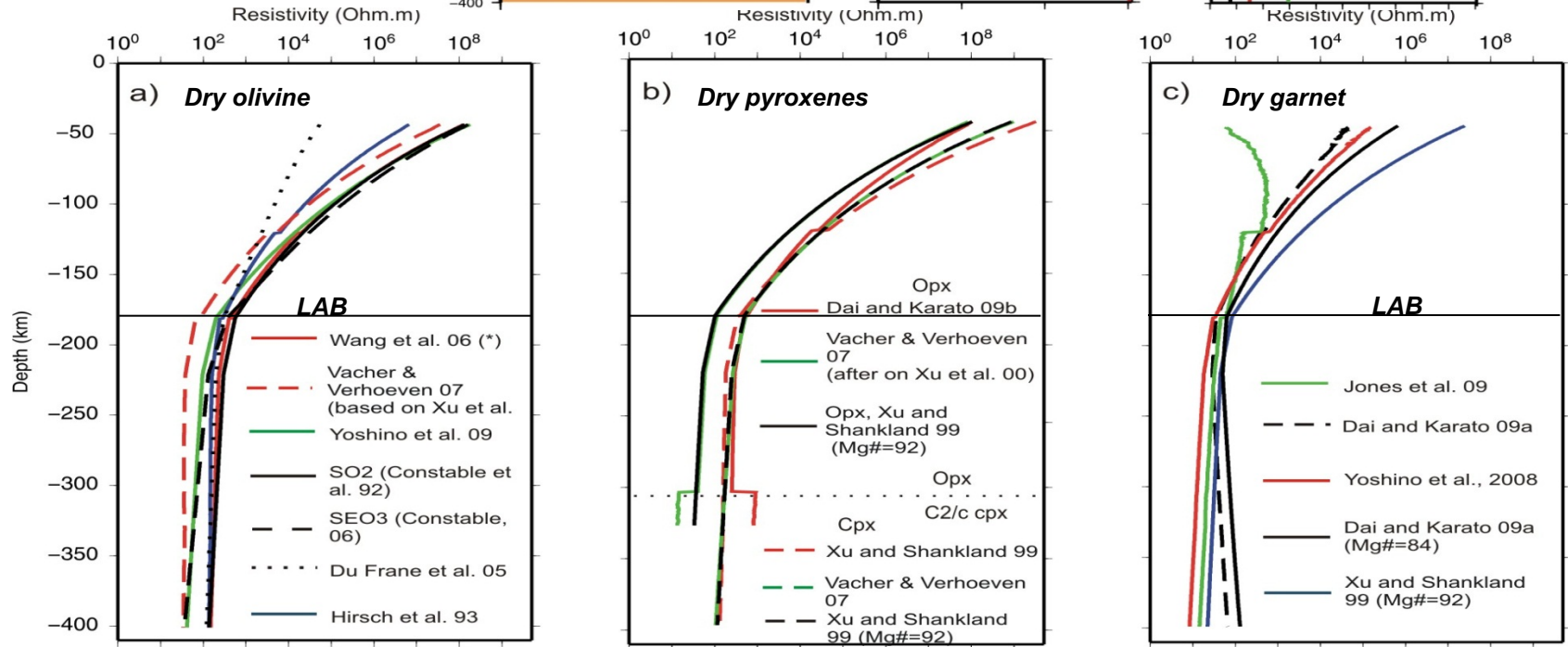
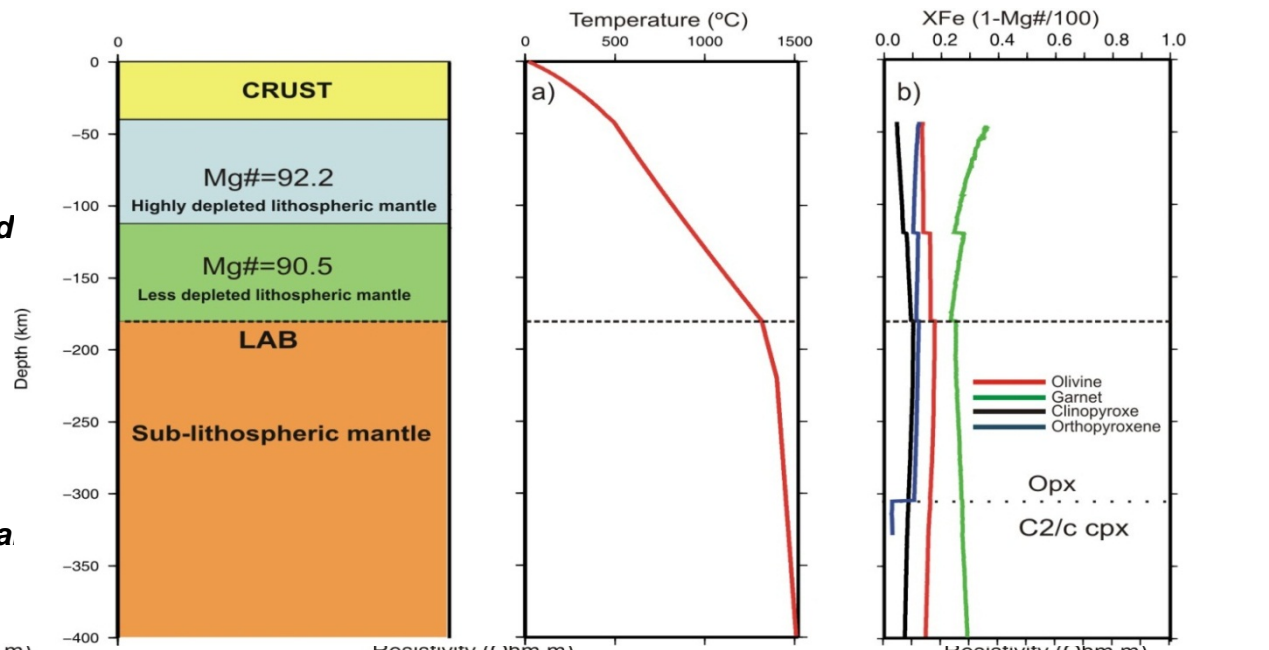
S. Heat flow=38-45 mW/m²

Electrical conductivity of the upper mantle: lab mineral studies (dry)

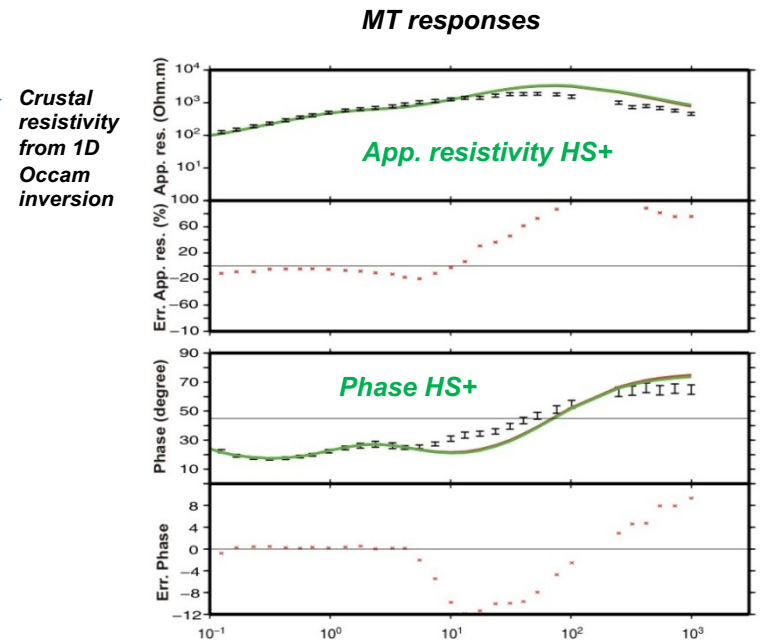
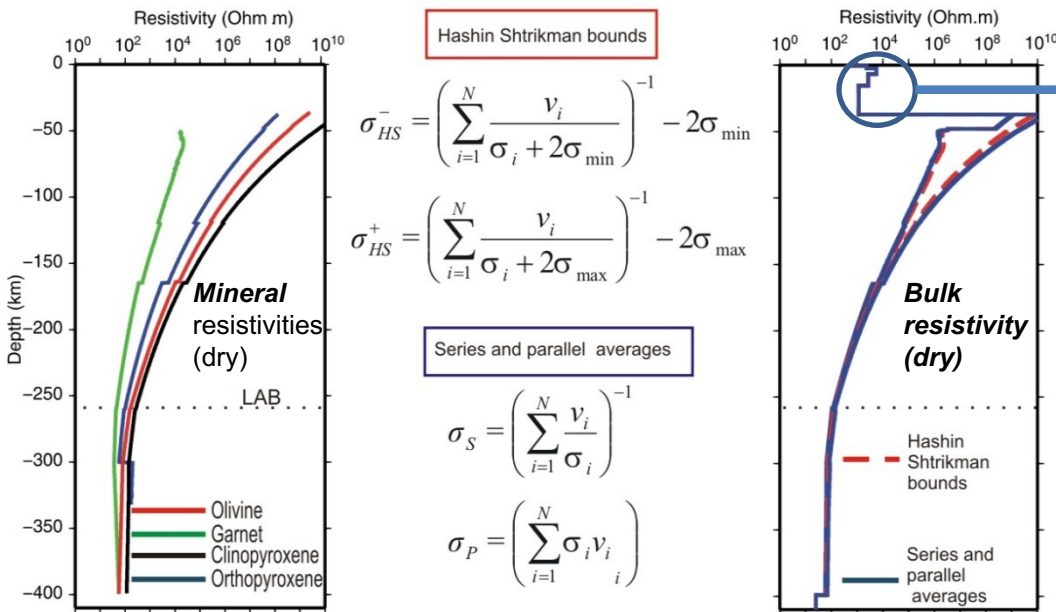
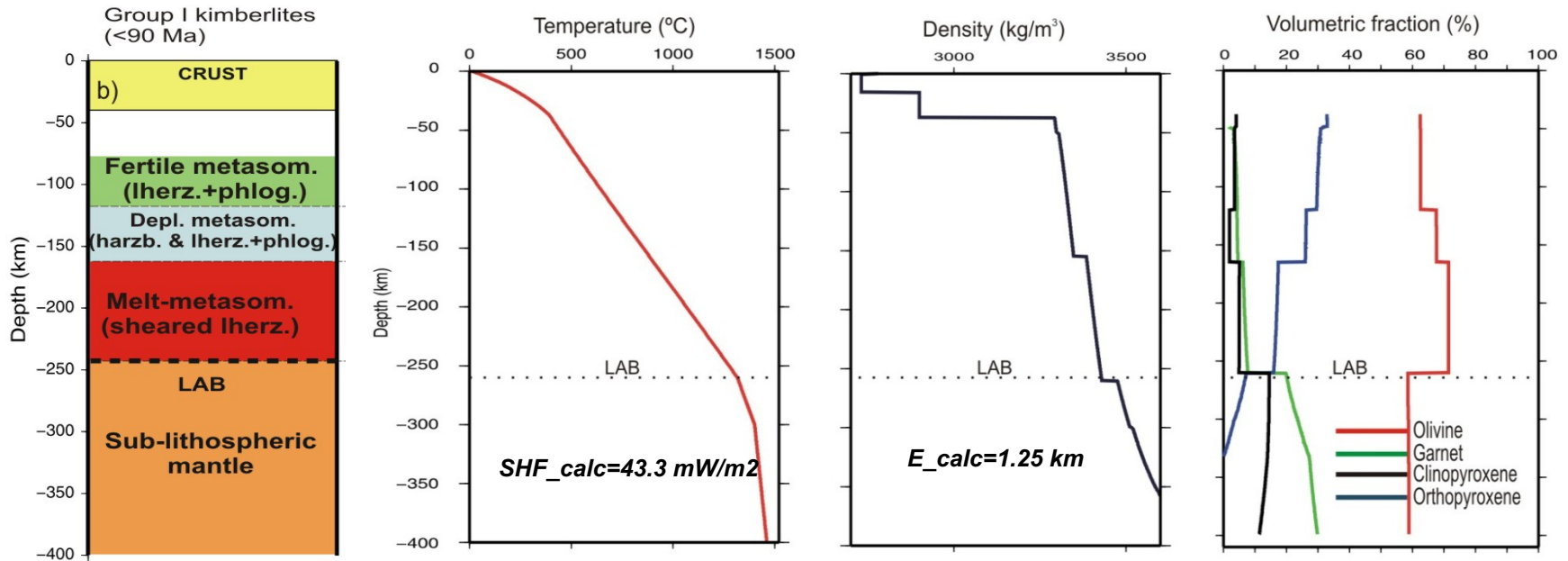
The electrical conductivity of upper mantle minerals accord to lab experiments:

*** Depends strongly on temperature**

*** Composition and pressure a second order effects**



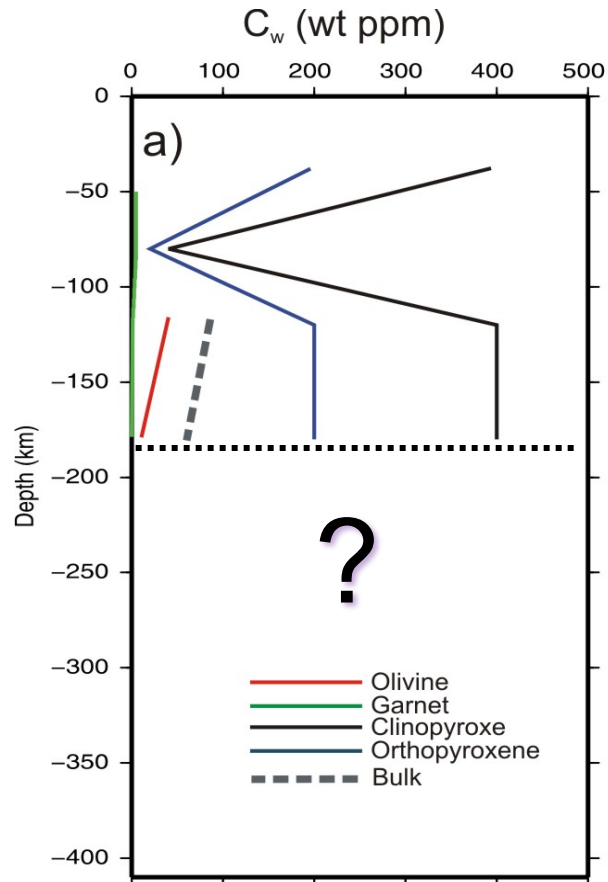
Electrical conductivity of the upper mantle: Kaapvaal (dry)



Crustal resistivity from 1D Occam inversion

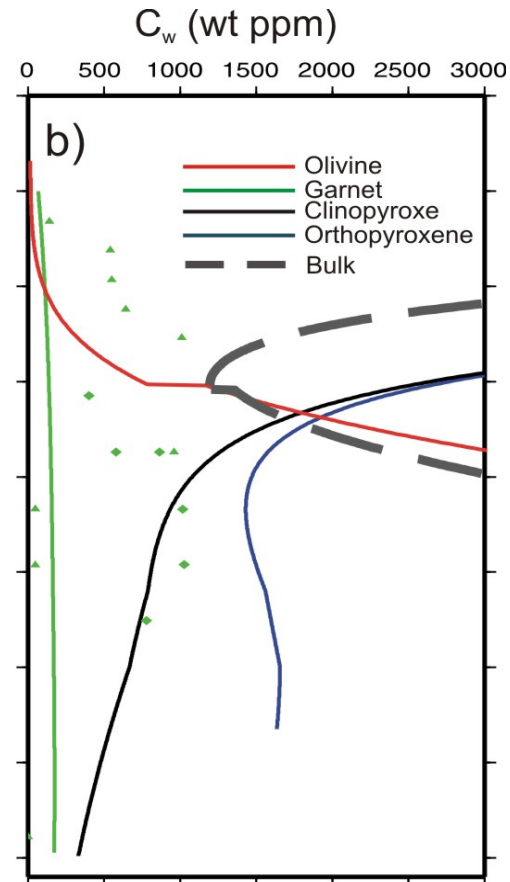
Electrical conductivity of the upper mantle: water content

Water content measurements from xenoliths, Kaapvaal craton



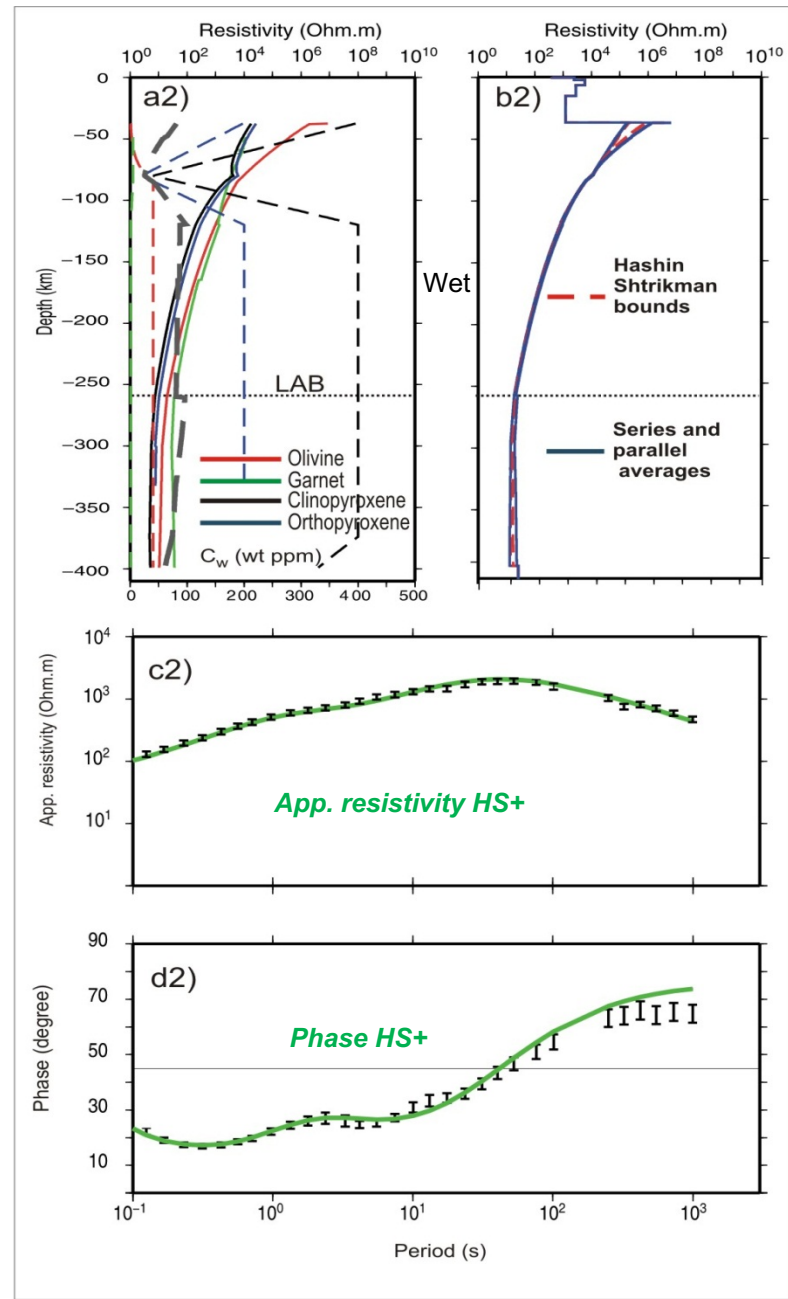
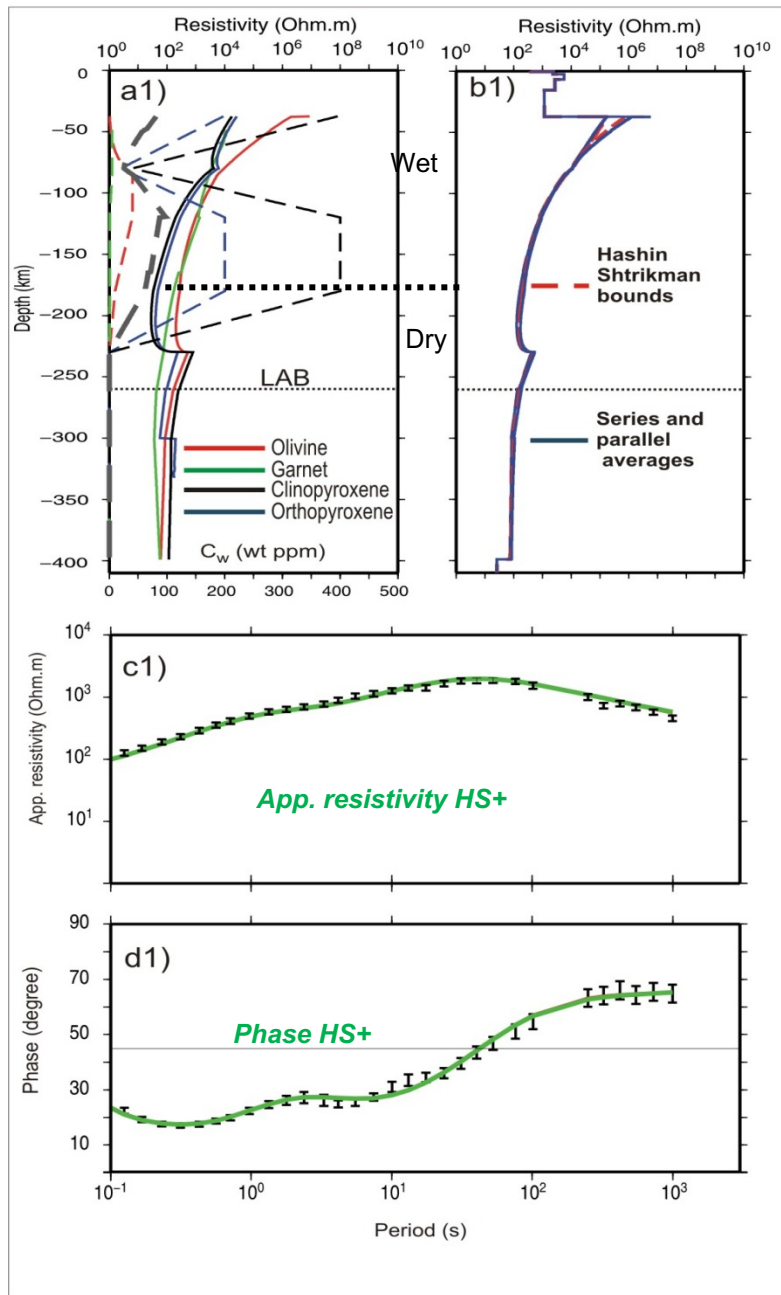
(Peslier, 2009; Grant et al., 2007)

Water solubility from lab studies

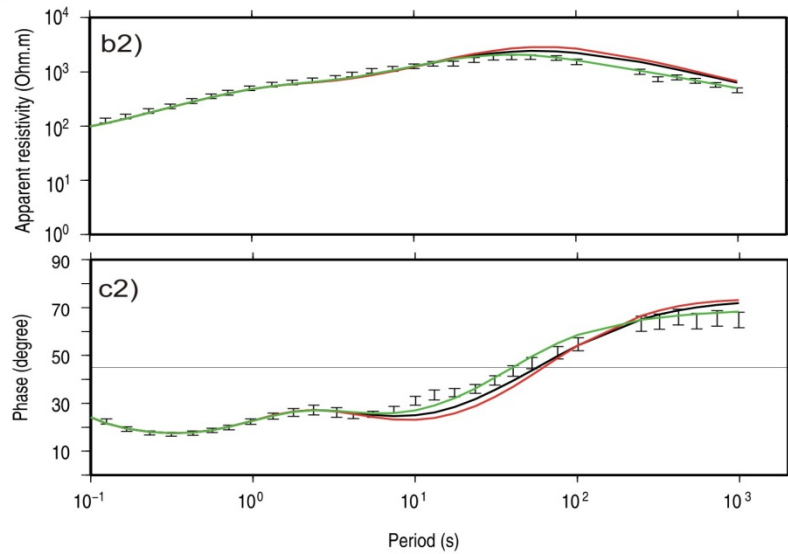
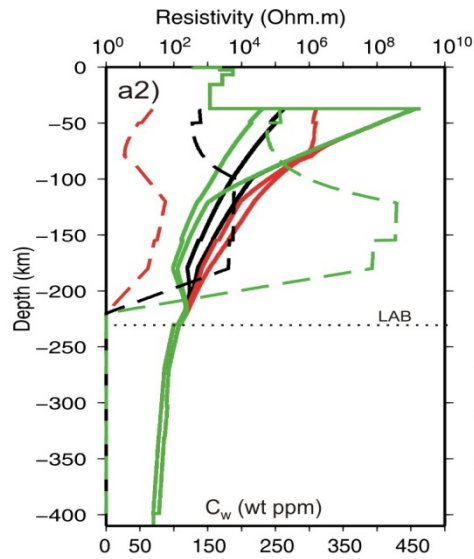


(Zhao et al., 2004; Mierdel et al., 2007; Gavrilenko, 2008; Lu and Keppler, 1997)

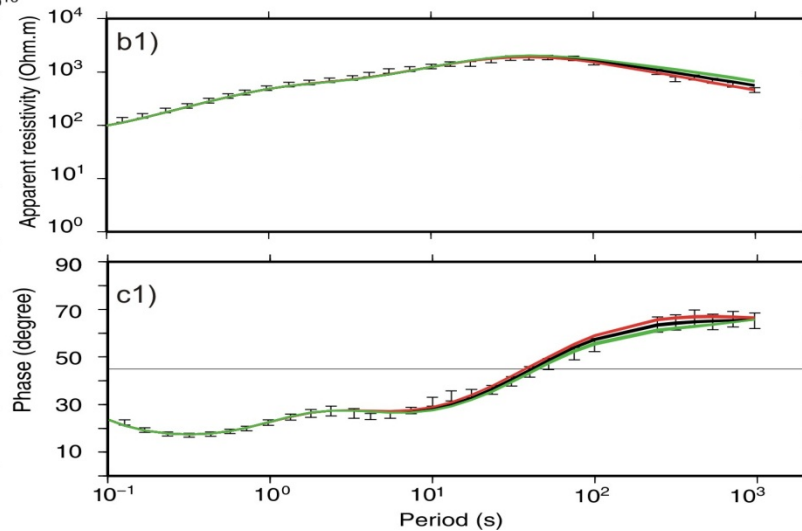
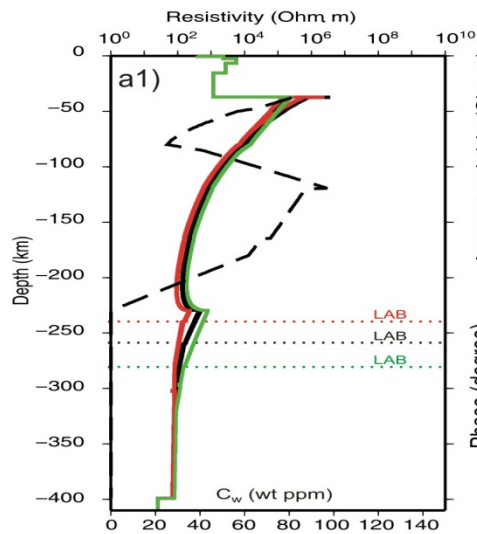
Electrical conductivity of the upper mantle: Kaapvaal (wet)



Electrical conductivity of the upper mantle: Sensitivity tests

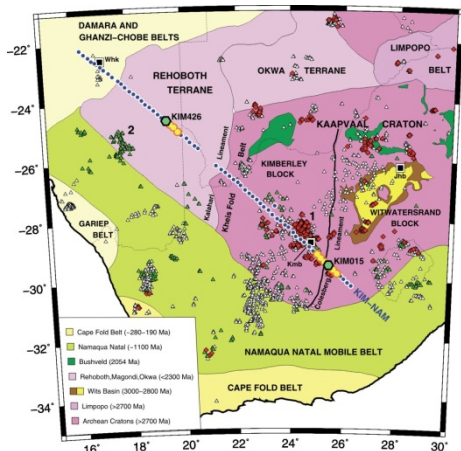


Water content upper most lithospheric mantle: 60-450 ppm



Lithosphere-asthenosphere boundary depth (thermal): 230-260 km

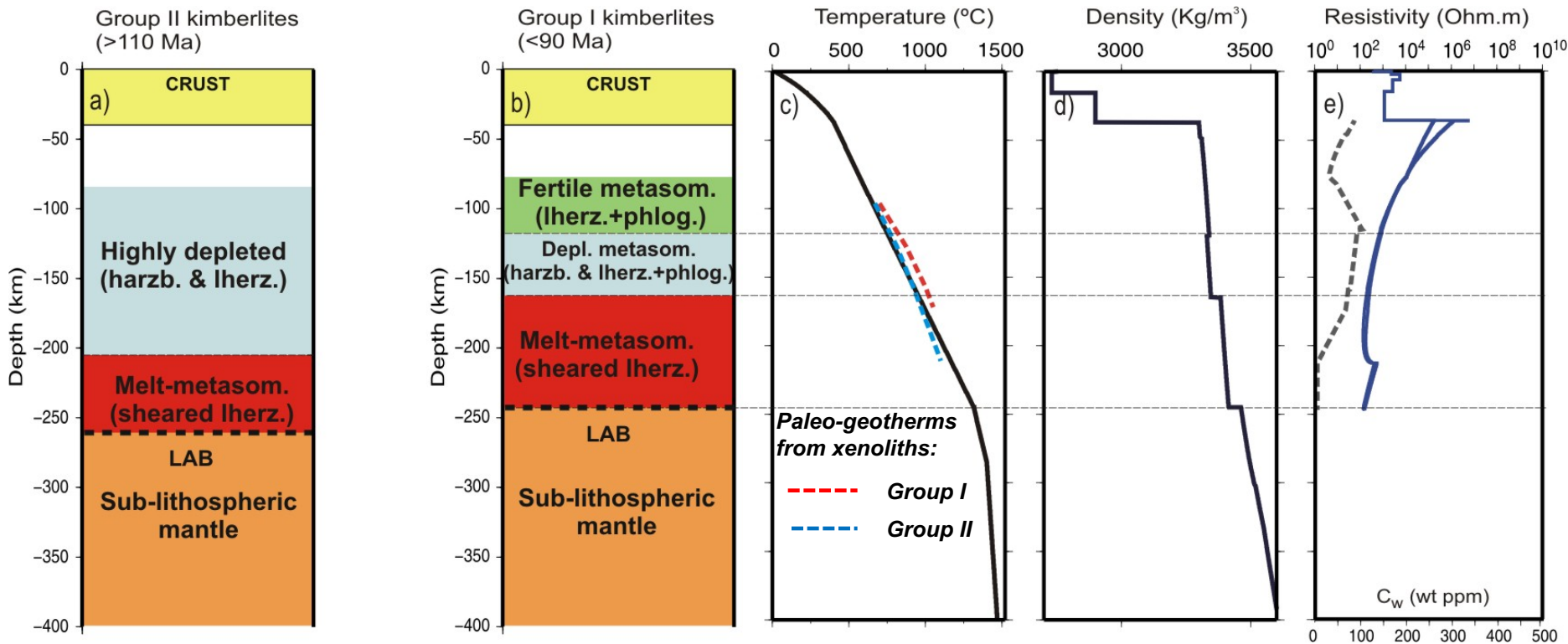
Kimberley block, Kaapvaal craton



Concluding remarks:

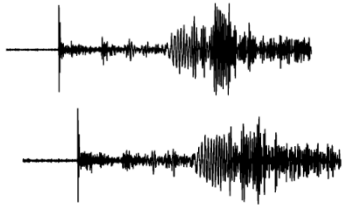
* Thermal LAB (230-260 km) consistent with previous seismic and 2D MT studies.

* Map water content in the lithosphere: wet upper most metasomatized and harburgitic layers, dry melt-metasomatized sheared lherzolites in the lower lithosphere.

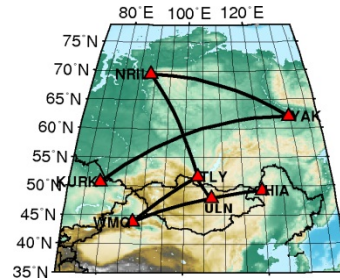


***Integrated modelling surface wave data
(Central Mongolia)***

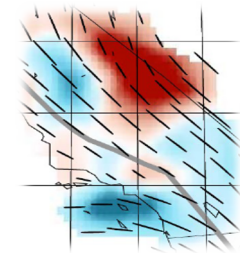
LitMod1D : Surface waves



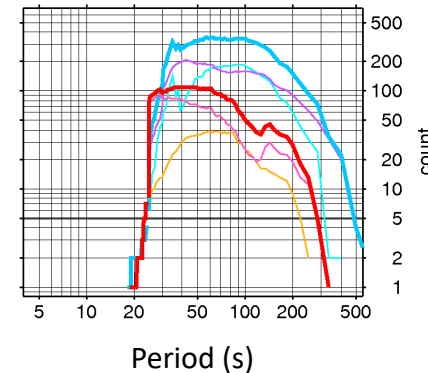
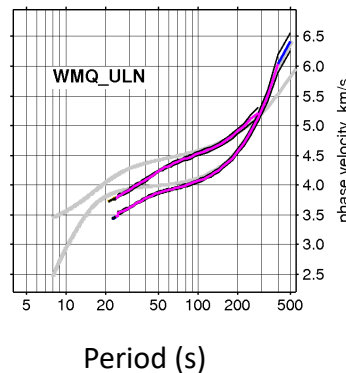
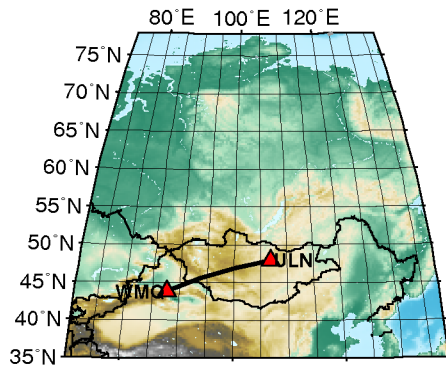
seismograms



inter-station, array measurements

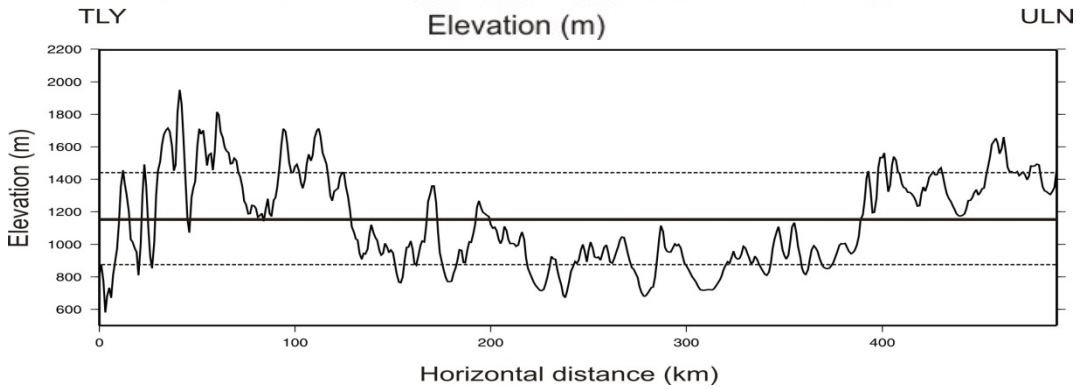
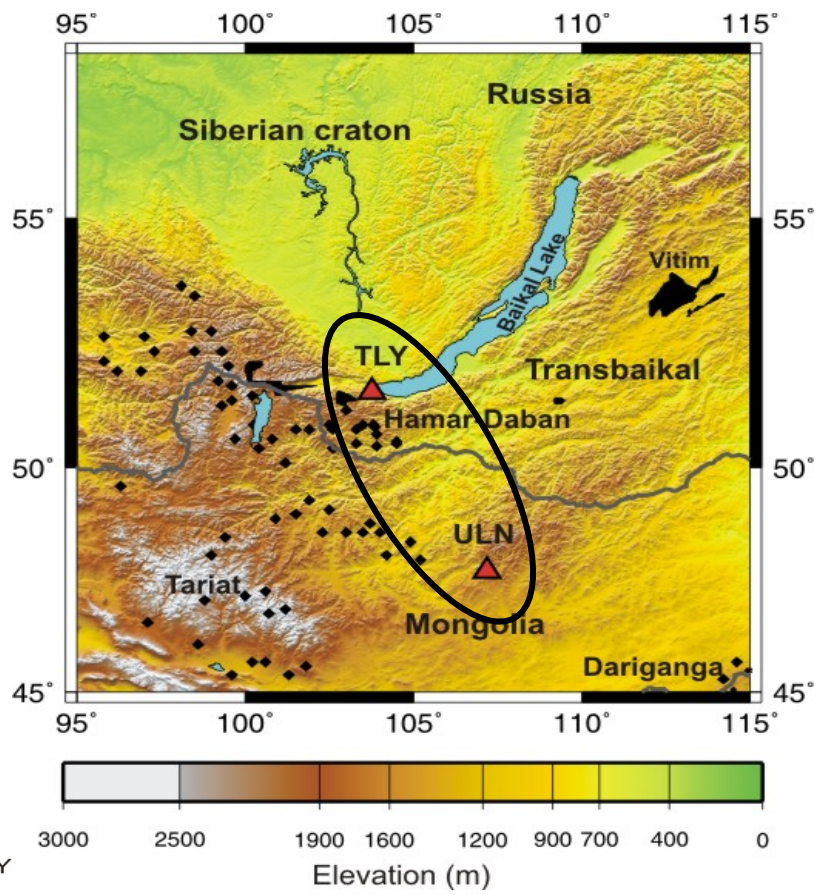


high-resolution regional tomography



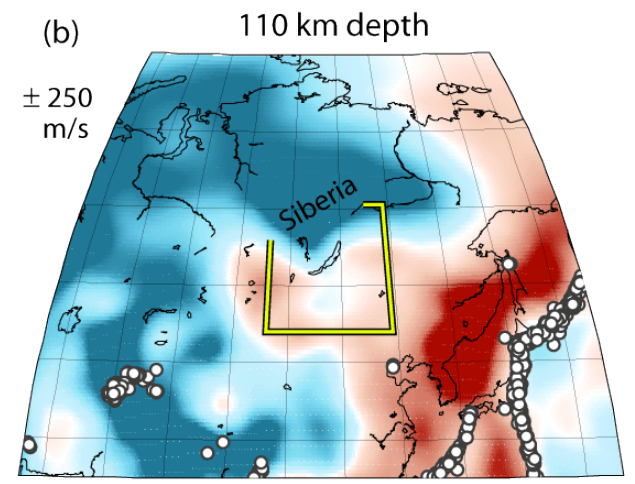
Pairs of stations, detailed dispersion curves

North Central Mongolia



Mantle composition

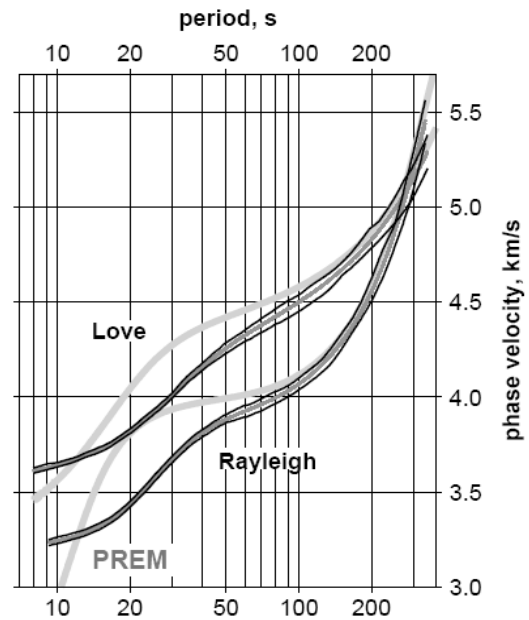
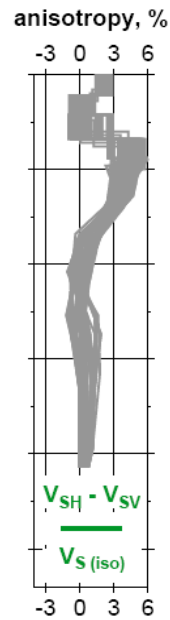
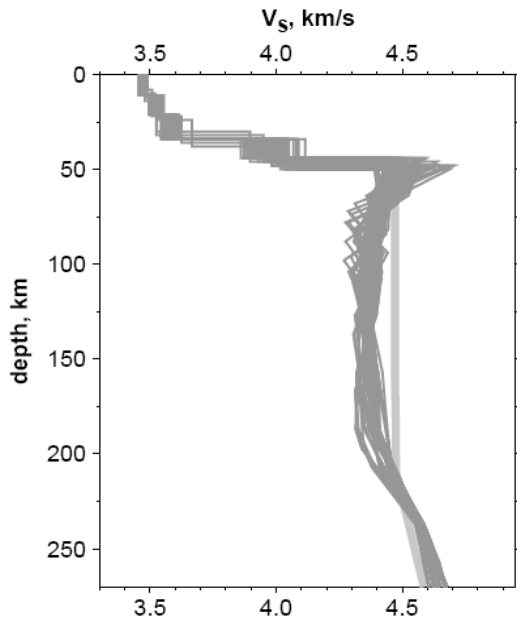
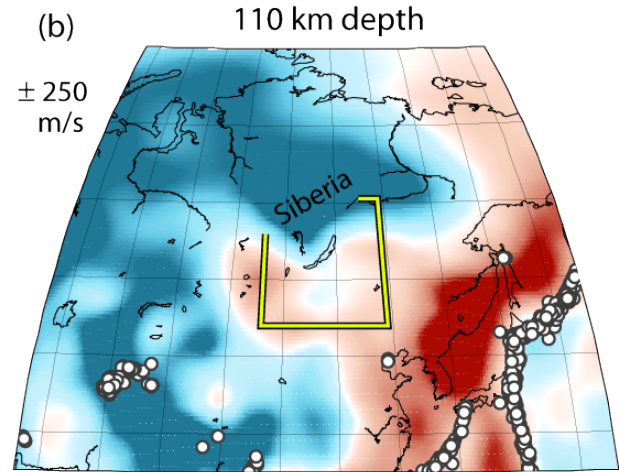
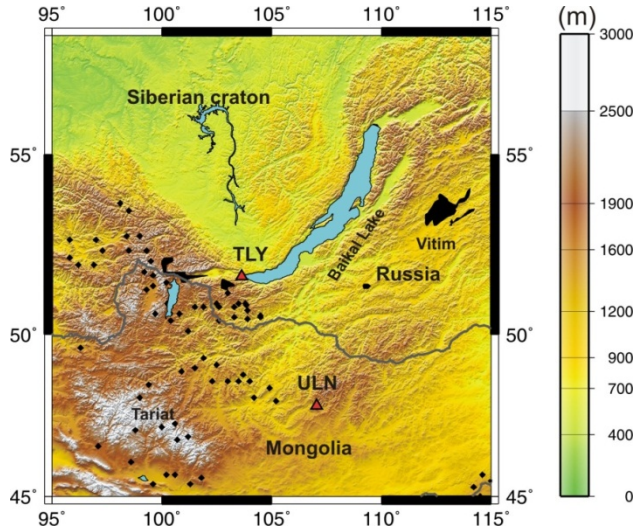
	a) Aver. Central Mongolia and Baikal	b) PUM M&S95
SiO ₂	44.59	45
TiO ₂	0.14	0.2
Al ₂ O ₃	3.48	4.5
Cr ₂ O ₃	0.4	0.38
FeO	8.25	8.1
MnO	0.14	0.14
MgO	39.56	37.8
CaO	2.85	3.6
Na ₂ O	0.31	0.36
Mg#	89.7	89.3



Lebedev et al. EPSL 2006

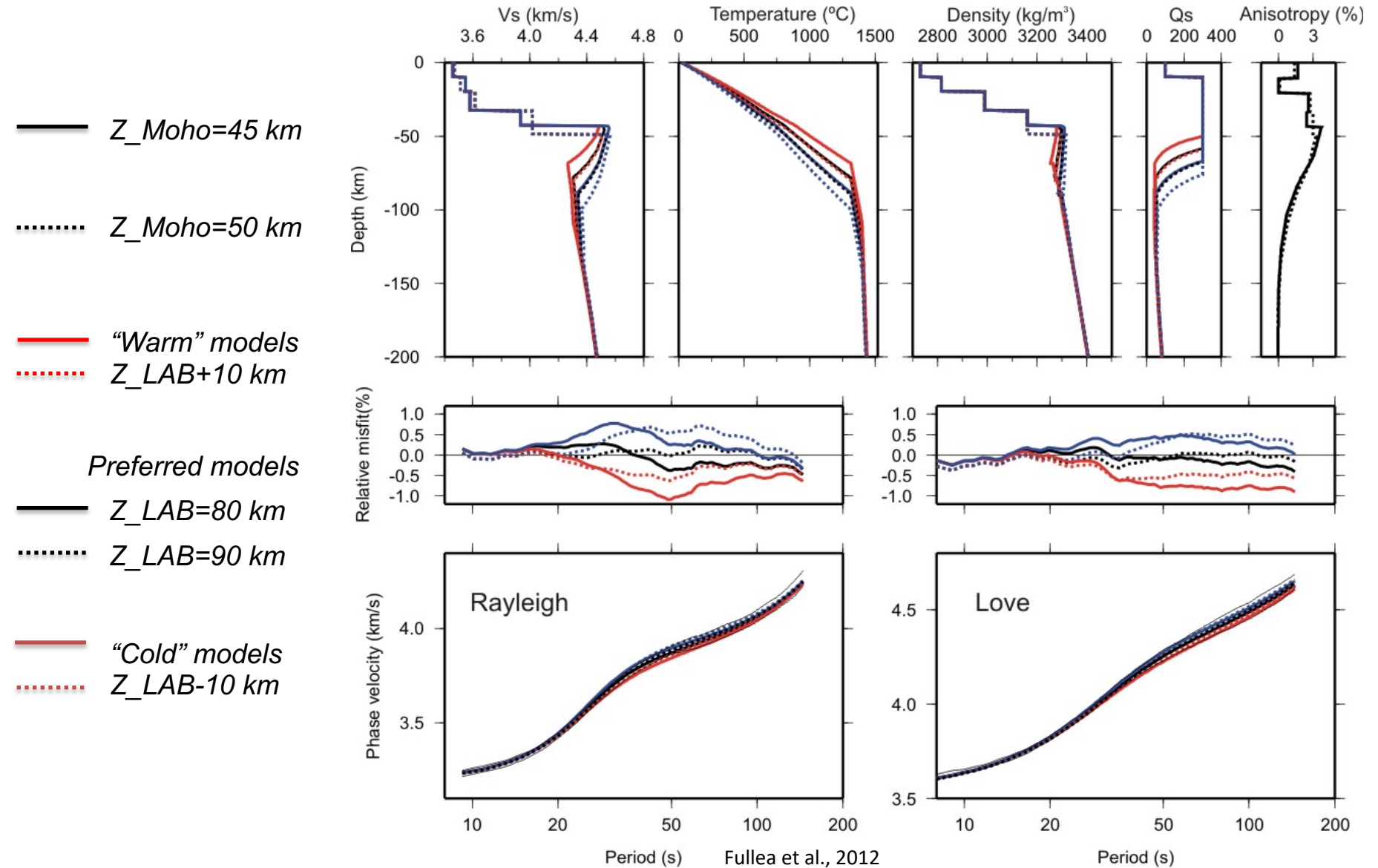
Surface wave seismic tomography

(Purely) Seismic models

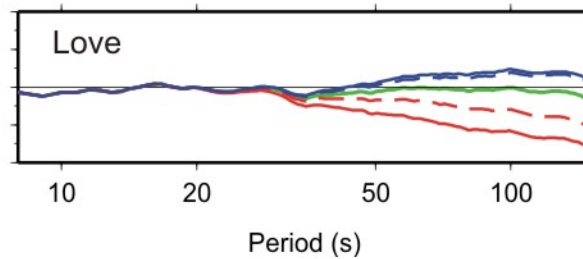
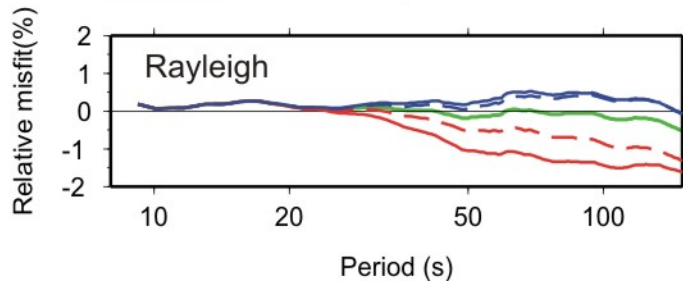
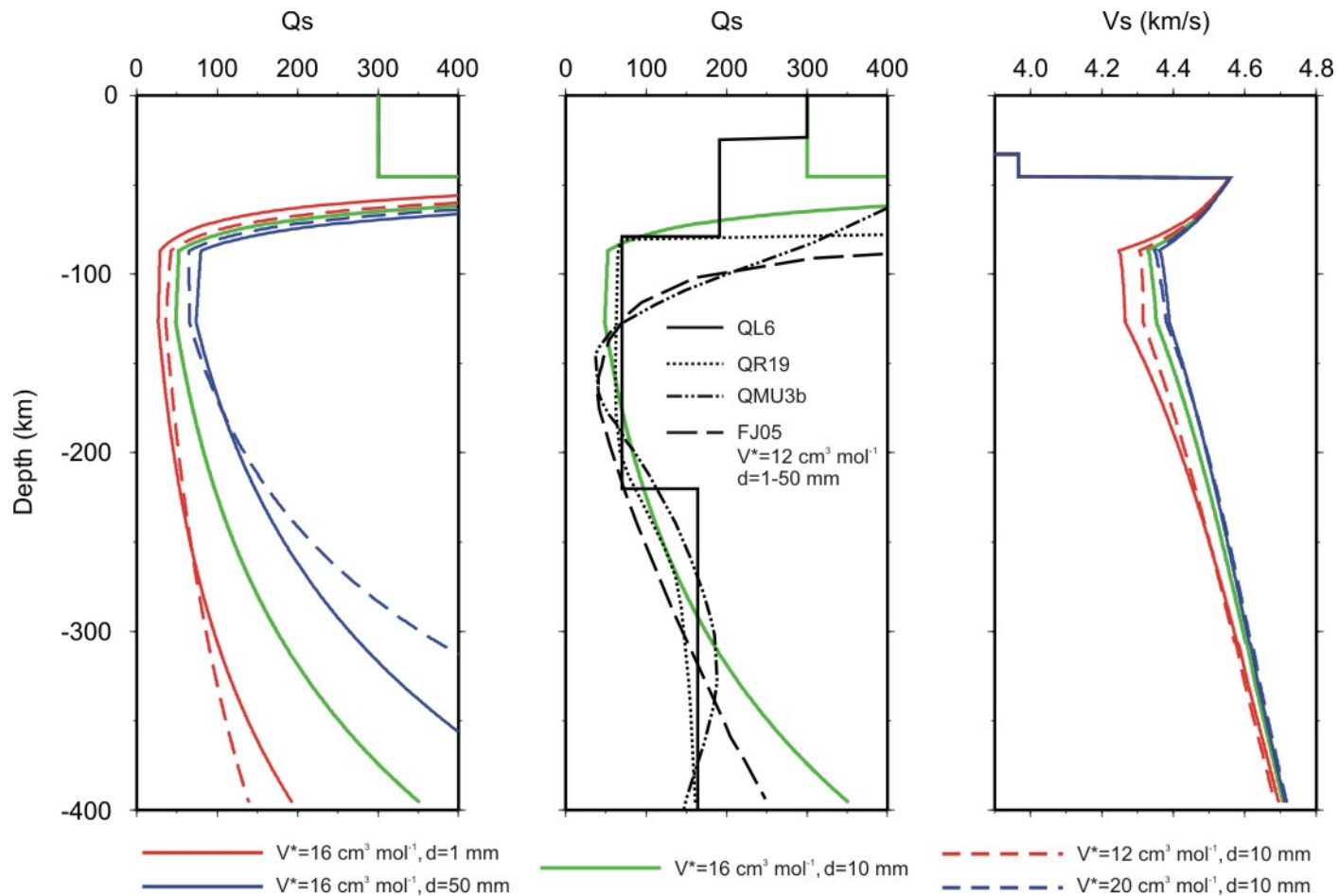


Range of plausible seismic models fitting surface wave data with relative error < 0.1%

Range of preferred models fitting surface wave data. Seismic velocities and densities computed as function of T , P and composition (LitMod)



Seismic attenuation

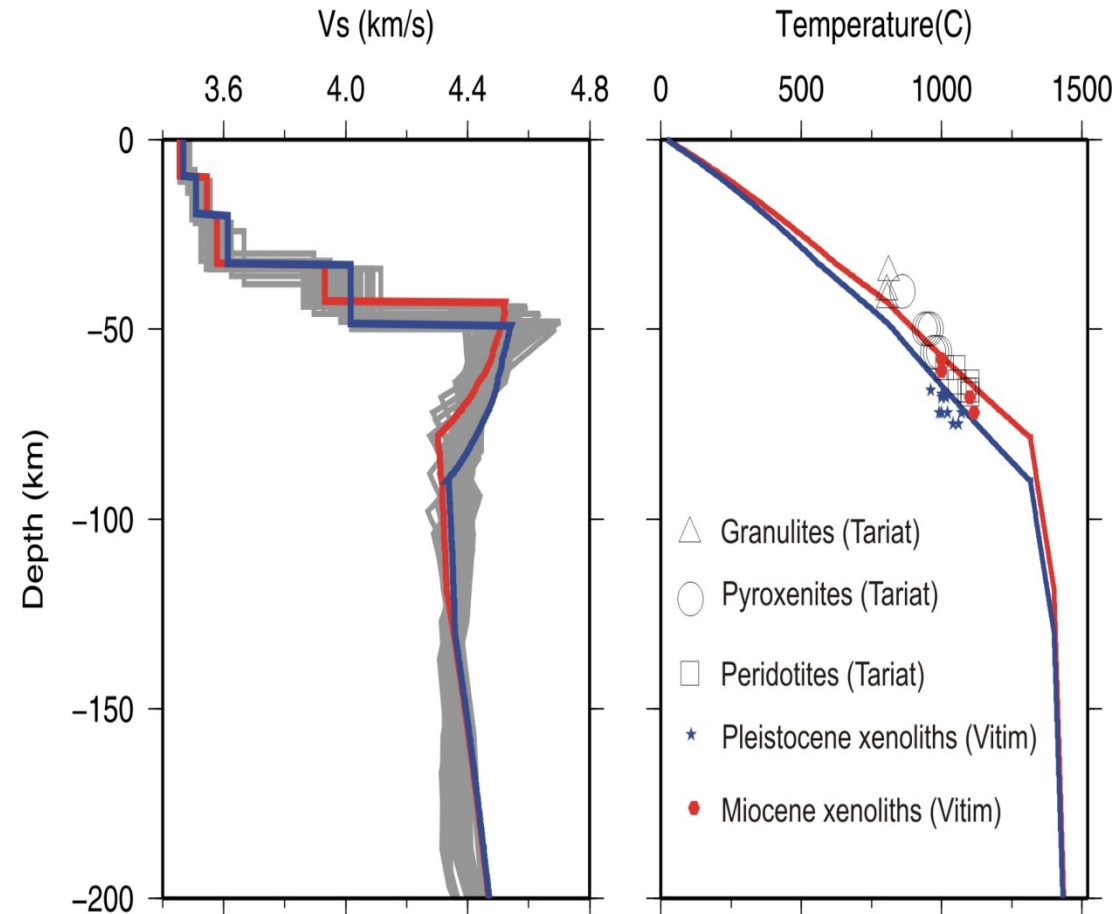


Integrated inversion: Xenolith data

Preferred integrated models

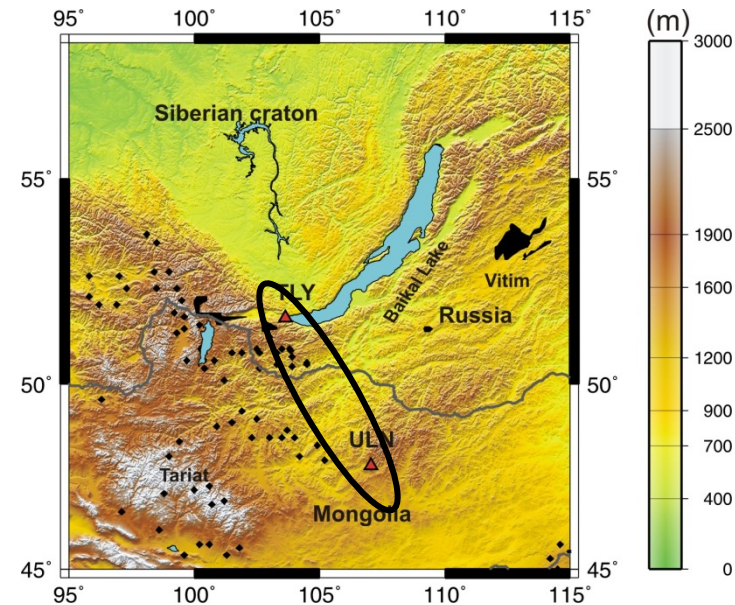
— $Z_{\text{Moho}}=45 \text{ km}, Z_{\text{LAB}}=80 \text{ km}$

— $Z_{\text{Moho}}=50 \text{ km}, Z_{\text{LAB}}=90 \text{ km}$



→ Integrated modelling effectively reduce the uncertainties of purely seismic inversions

→ Thermobarometric estimates from Cenozoic mantle xenoliths in central Mongolia confirm estimated geotherms



Summary of results

- 80-90 km LAB
- dense and mafic lower crust
- fertile-moderately depleted lithospheric mantle
- isostatically compensated topography

➤ Surface-wave sensitivity kernels

